Diploma thesis

In vivo investigation of corrosion kinetics and corrosion reactions between co-implanted durable materials and bioresorbable magnesium implants

submitted by

Melanie Lisa Napetschnig

to attain the academic degree

Doktorin der Zahnmedizin

(Dr.med.dent.)

at the

Medical University of Graz

conducted at the

University Clinic for Dental Medicine and Oral Health,

Departement of Oral Surgery and Orthodontics

under the supervision of

Assoz. Prof. Priv.-Doz. Dr.med.univ. Dr.med.dent.et scient.med.

Michael Payer

and

Dr. med.dent. Valentin Herber

Graz, July 14th, 2022

Declaration on oath

I hereby declare on my honour that I have written this thesis independently and without any unauthorised assistance from third parties and that I have not used any other sources than those indicated. All used sources used are thus marked as such and are evidenced by complete references in the text.

Graz, July 14th, 2022 Melanie Lisa Napetschnig e.h.

Acknowledgement

Hiermit möchte ich mich bei Hr. Assoz. Prof. Priv.-Doz. Dr.med.univ. Dr.med.dent.et scient.med. Michael Payer für die Betreuung bei der Erstellung dieser Arbeit bedanken.
Mes remerciements vont également à M. Dr. med.dent. Valentin Herber pour son aide infatigable lors de la rédaction de mon premier travail scientifique. Merci beaucoup !

Mein größter Dank gilt meiner Familie. Mama, Papa, Omi und Bettina. Ohne eure Unterstützung und Liebe wäre es mir nicht möglich gewesen dieses Studium zu bestreiten. Danke dafür, dass ihr mich stets hingebungsvoll bei all meinen Träumen unterstützt.

S., auch dir möchte ich danken, dass du immer bedingungslos an meiner Seite stehst. Jeg elsker deg.

Danke auch an meine Studienkolleg*innen für die unvergessliche Studienzeit.

Table of Contents

List of abbreviations

Al ..... Aluminium
bw ..... body weight
BIC ..... Bone Implant Contact
Ca ..... Calcium
et al. ..... Et alii
GPa ..... Gigapascal
g ..... Gram
HU ..... Hounsfield
H_2 ..... Hydrogen gas
OH^- ..... Hydroxide ions
i.e. ..... Id est
Fe ..... Iron
Mg ..... Magnesium
Mg^{2+} ..... Magnesium ions
Mn ..... Manganese
µm ..... Micrometers
µCT ..... micro-computed tomography
mg ..... Milligram
mm ..... Millimeter
Nd ..... Neodym
cp-Ti ..... Pure titanium
REE ..... Rare Earth Elements
resp. ..... Respectively
Ag ..... Silver
s.c. ..... subcutaneous
Ti ..... Titanium
V ..... Vanadium
wt ..... Weight
Y ..... Yttrium
Zn ..... Zinc
Zr ..... Zirconium

List of figures

List of tables

List of formulas

Zusammenfassung

Einleitung: Ziel dieser Studie war es, eine *in vivo* Untersuchung bezüglich der Korrosionskinetik und Reaktionen bei Koimplantation von dauerhaften Materialien wie Titan (Ti) und bioresorbierbarem Magnesium (Mg) durchzuführen, um folglich deren gegenseitigen Einfluss hinsichtlich Materialeigenschaften und Degradationsrate zu evaluieren und quantifizieren.

Die Anwendung von bioresorbierbarer Implantationsmaterialien konnte in den letzten Jahrzehnten sowohl in der pädiatrischen Chirurgie und Traumotologie als auch in der zahnmedizinischen Chirurgie und Implantologie an Interesse gewinnen. Zurückzuführen ist dies auf deren positiven Materialeigenschaften wie beispielsweise der hervorragenden Biokompatibilität und Osseointegration sowie deren guten mechanischen Eigenschaften. So kann es jedoch bei einer Koimplantation aufgrund des unterschiedlichen elektrochemischen Potenzials der Metalle und der daraus resultierenden Bildung einer galvanischen Zelle zur Beschleunigung der Degradationsgeschwindigkeit kommen. Jenes unbeständige und teils unvorhersehbare Korrosionsverhalten wird als limitierender Faktor für die Anwendung von bioresorbierbaren Mg als Alternative zu herkömmlichen Implantationsmaterialien diskutiert.

Material und Methoden: Im Rahmen eines chirurgischen Eingriffes kam es bei zwei Versuchsgruppen zu einer bilateralen transkortikalen Koimplantation von Pins (ø= 1.4 mm, h= 6 mm) aus einer Mg-basierten Metalllegierung (ZX00) und Ti-6Al-4V (Titan Grad 5) in die Tibiae der männlichen Versuchstiere, 24 Spraque-Dawley® (SD) Ratten, mit einem Abstand von 5 und 10 mm.

Der Kontrolle dienend, kam es bei zwei weiteren Gruppen von Versuchstieren zu einer Sham-Operation und somit zu einer Bohrung in den Knochen ohne Insertion eines Titanpins. Es wurden am Tag der Implantation sowie 4, 8 und 12 Wochen post implantationem Mikro CT (µCT) Bilder der implantierten Pins angefertigt. Anschließend wurden diese durch die Verwendung der Bildverarbeitungssoftware MIMICS Software, Version 23.0 als dreidimensionale Darstellungen rekonstruiert. Es folgte eine Quantifizierung des durch die Korrosion entstandenen

Wasserstoffgases (H_2) sowie die der Veränderungen der Implantatoberflächen und der Implantatvolumina.
Ebenso wurde eine qualitative histologische Evaluierung mittels Methylenblau und basischem Fuchsin durchgeführt. Zu verschiedenen Zeitpunkten (T 0, W 4, W 8 und W 12) wurde für dasselbe Material eine statistische Analyse mittels Einweg-Varianzanalyse (ANOVA) durchgeführt.

Ergebnisse: Wir konnten eine moderate Wasserstoffgasentwicklung über den gesamten Versuchszeitraum von zwölf Wochen in all unseren Versuchsgruppen verzeichnen. Lediglich in der Gruppe mit der Distanz von 5 mm zwischen den ko-implantierten ZX00 sowie Ti Pins wiesen die Ergebnisse unserer µCT-Analysen eine geringgradig höhere H_2 gas Produktion auf. Die von uns beobachtete initiale Zunahme des Implantatvolumens und der Oberfläche, konnte auf die Bildung der in der Literatur beschriebenen Korrosionsschicht auf den ZX00 Oberflächen zurückgeführt werden. Die Messungen des longitudinalen Knochenwachstums ergaben ebenfalls eine homogene Zunahme in allen Versuchsgruppen.

Konklusion: Die Ergebnisse unserer *in vivo* Studien zeigen keinen Einfluss von Ti auf die Degradation des bioresorbierbaren ZX00 durch die galvanische Korrosion bis zu 12 Wochen nach der Implantation. Ebenso konnte nachgewiesen werden, dass es zu keiner Beeinträchtigung des longitudinalen Knochenwachstum kam, was ZX00 zu einer vielversprechenden bioresorbierbaren Alternative im Bereich der pädiatrischen Chirurgie und Orthopädie.
Um das Abbauverhalten bis hin zur völligen Auflösung von ZX00-Stiften beurteilen zu können, müssen jedoch weitere In-vivo- und klinische Untersuchungen durchgeführt werden.

Abstract

Introduction: The aim of this study was to perform an *in vivo* investigation of the corrosion kinetics and reactions during co-implantation of durable materials such as titanium (Ti) and bioresorbable magnesium (Mg) in order to consequently evaluate and quantify their mutual influence on material properties and degradation rate. The use of biodegradable implantation materials has gained interest in recent decades in paediatric surgery and traumatology as well as in dental surgery and implantology. This is due to their positive material properties such as excellent biocompatibility and osseointegration as well as their good mechanical properties. However, co-implantation can accelerate the rate of degradation due to the different electrochemical potential of the metals and the resulting formation of a galvanic like cell. This unstable and partly unpredictable corrosion behaviour is discussed as a limiting factor for the application of bioresorbable Mg as an alternative to conventional implantation materials.

Methods: During a surgical procedure, bilateral transcortical co-implantation of pins (ø= 1.4 mm, h= 6 mm) made of a Mg-based metal alloy (ZX00) and Ti-6Al-4V (titanium grade 5) occurred in the tibiae of 24 male Spraque-Dawley® (SD) rats at 5 and 10 mm. Furthermore, as a control, magnesium spaced by shams were implanted in a group of experimental animals.
µCT scans of the implanted pins were taken on the day of implantation and at 4, 8 and 12 weeks post-implantation to quantify the hydrogen gas produced by corrosion and the rate of degradation and to detect changes in the implant surface and volume. A qualitative histological evaluation was also performed using methylene blue and basic fuchsin. At various times (T 0, W 4, W 8 and W 12) of the same material, statistical analysis using one-way-analysis of variance (ANOVA) was carried out.

Results: We observed a moderate hydrogen gas production in all our experimental groups over the entire experimental period of twelve weeks. Only in the group with the distance of 5 mm between the co-implanted ZX00 and Ti pins did the results of our µCT analyses show a slightly higher H_2 gas production compared to the rest of

the experimental groups. The initial increase in implant volume and surface area we observed could be attributed to the formation of the corrosion layer on the ZX00 surfaces described in the literature. The measurements of longitudinal bone growth also showed a homogeneous increase in all test groups.

Conclusion: The results of our *in vivo* studies show no influence of Ti on the degradation of bioresorbable ZX00 due to galvanic corrosion up to 12 weeks after implantation. Furthermore, it could be shown that there was no impairment of longitudinal bone growth, making ZX00 a promising bioresorbable alternative in the field of paediatric surgery and orthopaedics. To estimate the degrading behaviour up to the total dissolution of ZX00 pins, however, more *in vivo* and clinical research must be done.

1 Introduction

Different types of implants are already in clinical use in dentistry, more precisely dental implantology, orthopedics as well as trauma and paediatric surgery.
In recent years, however, the usage of bioresorbable Mg implants in the field of orthopedics, paediatric and trauma surgery have proven to be an excellent alternative to conventional durable implantation materials such as titanium.
Especially because of their outstanding properties such as a density and elastic modulus approximately similar to the bone, excellent osseointegration and osteoconductivity as well as biocompatibility.
Thus, the so-called stress shielding effect is also minimised by the elasticity mode (e-modulus), which is similar to that of bone. The so-called e-modulus represents a reference value for the existing stiffness of a material.
The advantage of using bioresorbable implant materials such as Mg is that they are gradually dissolved and absorbed in the human body. Therefore, eliminating the need for a second surgical procedure to remove the implant and therefore reduce the risk of developing comorbidities.
However, co-implantation of Ti and Mg can lead to corrosion due to their opposite electrochemical potential in the galvanic series, which can sometimes have a reciprocal effect on their material properties and degradation.
This corrosion reaction can result in strong hydrogen gas (H_2) evolution and following release to the surrounding tissue, pH changes and Mg ion release. In order to prevent the disadvantages of too rapid degradation, modifications and changes can be made to the implant surface or the alloy composition can be changed (1-8).

Investigations into Mg as an implantation material for medical use began as early as 1898 by the Austrian physician Erwin Payr. Another pioneer in this field of research was the Belgian physician and scientist Albin Lambotte.
In 1902, Lambotte carried out a fixation of a lower leg (tibia) by inserting an Mg disk and six further screws made of steel. In this patient, massive subcutaneous swelling associated with pain was observed as a result of too rapid H_2 gas evolution. Due to the unsolved problem of the Mg corroding too rapidly, the use of metallic materials,

such as titanium and steel, was preferred from the middle of the 19th century to the beginning of the 20th century because of their stable mechanical properties. In today's literature, studies on the clinical application of Mg as a bioresorbable implantation material can already be found. Nevertheless, it is of relevance to investigate this material especially with regard to a potential co-implantation with another material and its long-term effect (2, 9, 10).

1.1 Dental implantology materials

Current materials used in dental implantology and especially in bone tissue engineering can be divided into different categories.
As shown in figure 1, one way to classify these materials would be in terms of their chemical background. Dental implantology materials can be classified into ceramics (zirconia and alumina), metals (steel and titanium) and polymers (11-13).

Table 1 Select biomaterials classified by material type with examples of their application in medical devices

Classification	Biomaterial	Examples of applications
Metal	316L stainless steel	Surgical instruments, orthopedic fixation devices, stents
Metal	Titanium and titanium-containing alloys	Fracture fixation, pacemaker encapsulation, joint replacement
Metal (shape memory alloy)	Nickel–Titanium Alloy (Nitinol)	Stents, orthodontic wires
Metal	Platinum and platinum-containing alloys	Electrodes
Metal	Silver	Anti-bacterial material
Polymer	Polytetrafluoroethylene (PTFE, Teflon®, Gore-Tex®)*	Vascular grafts, catheters, introducers
Polymer	Poly(ethylene terephthalate) (polyester, Ethibond, Dacron®)	Vascular graft, drug delivery, non-resorbable sutures
Polymer	Poly(methyl methacrylate) (PMMA)	Bone cement, intraocular lens
Polymer	Polyurethane	Catheters, tubing, wound dressing, heart valves, artificial hearts
Polymer	Silicone rubber (polydimethylsiloxane PDMS)	Catheters, feeding tubes, drainage tubes, introducer tips, flexible sheaths, gas exchange membranes
Polymer	Polycarbonate	Major component in renal dialysis cartridge, heart-lung machine, trocars, tubing interconnectors
Polymer	Hydrogels (poly(ethylene oxide), poly(ethylene glycol), poly(vinyl alcohol), etc.)	Drug delivery, wound healing, hemostasis, adhesion prevention, contact lenses, extracellular matricies, reconstruction
Polymer	Polyamides (nylon)	Non-resorbable sutures
Polymer	Polypropylene (ie, prolene)	Non-resorbable sutures, hernia mesh
Ceramic	Alumina	Joint replacement, dental implants, orthopedic prostheses
Ceramic	Carbon	Heart valves, biocompatible coatings, electrodes
Ceramic	Hydroxyapatite	Implant coatings, bone filler
Ceramic	Bioglass	Metal prostheses coating, dental composites, bone cement fillers

*Teflon and Dacron are trademarks of E. I. DuPont de Nemours & Co, and Gore-Tex is a trademark of W. L. Gore & Associates, Inc.

Figure 1: Biomaterials and their field of clinical application based on examples (13)

1.1.1 Need for bioresorbable materials in oral and orthognathic surgery

In oral surgery, existing bony defects such as horizontal and/or vertical bone resorption can be reconstructed by periodontal/surgical procedures using augmentations to provide sufficient stability for tooth replacement using implants.
The augmentations can be carried out with the help of different materials. On the one hand, a distinction is made between

i. Autogenous replacement material
ii. Allogenic replacement material
iii. Xenogenic replacement material
iiii. Alloplastic replacement material.

Whereby autogenous replacement material, i.e. material in which the donor and recipient are the same person, represents the gold standard due to the low risk of rejection and immune reaction. The most common way of obtaining autogenous replacement material is by intraoral harvesting, more precisely in the region of the ramus mandibulae (14-16). Collagen membranes are commonly used to cover those defects. These bioresorbable membranes serve as a barrier and restrict the ingrowth of epithelial tissue into the bony defect, thus allowing the bony healing of the defect to progress. In some clinical situation, the membranes are screw to the bone to fix it and to avoid any malposition of the membranes.
To the date, fixation screws made of Ti are used in the field of oral surgery. Promising studies have already been conducted using Mg screws as fixation materials in mandibular fractures.
Therefore, there is also a need for further research in the field of dentistry regarding the application of bioresorbable materials and especially regarding the use of a combination of different biomaterials such as Mg and Ti (17-19).

1.1.2 Ceramics

These biomaterials also have good biocompatibility and bioresorbability. In addition, they are non-toxic and non-immunogenic.
Therefore, they are commonly known for their clinical usage as bone grafts.
When considering ceramics in terms of the biological reaction they trigger in the tissue of the implant site, a distinction can be made between:

a. bioresorbable
b. bioinert
c. and biodegradable ceramic materials.

Bioresorbable as well as biodegradable materials are both capable to interact with the bone and the bone tissue. Over time, the degrading material is replaced by normal functional bone. With bioinert materials there is no biological interaction with the human body and consequently no rejection reactions occur. The ceramics are mostly made of tricalcium phosphate (alpha- and beta- TCP) or hydroxyapatite (HA). A distinction is made between the different crystalline forms Alpha-TCP (α) and Beta-TCP (β). Due to the instability and cytotoxicity that α-TCP exhibits, it is not considered relevant in clinical practice. β-TCP, has a chemical structure quite similar to bone's and therefore osseointegration and osteoconductive properties related to hydroxyapatite. The disadvantage of HA is its very slow degradation and resulting long retention in the body or insertion site.
Both ceramics made of pure hydroxyapatite and a two-phase hybrid of hydroxyapatite together with β-TCP find application in clinical use. Those so-called biphasic calcium phosphates find a wide range of applications mainly due to their biocompatibility and good osteoconductive potential.
The components of these biphasic calcium phosphates are both hydroxyapatite (HA) and beta-tricalcium phosphate (β-TCP), with a usual composition of 60 % HA and 40 % TCP usually being used. Like it is shown in the following figure 2, one of the advantages of ceramics is their porous structure which promotes osteoconductivity by ensuring a good supply of nutrients to the bone tissue that settles on the surface of the implants.
Another disadvantage is the unprevisible degradation rate, which can take a long time in certain cases.

The high stiffness and low fracture and tensile strength can be seen as a negative attribute and leads to the fact that an application in the load-bearing area is not considered sensible (13, 20-24).

Advantages	Disadvantages	Clinical application
□ Porous structure	□ Brittle □ Poor tensile strength	□ Bone-grafting material

Figure 2: Biodegradable polymers and its benefits and disadvantages (22)

1.1.3 Polymers

Polymers which are used in a variety of medical applications, such as orthopaedic fixation materials like pins or screws, are made from the raw material lactic acid. Among the most commonly used are polylactic acid (PLA), polyglycol acid (PGA) and polylactic glycol acid (PLGA).

The group of polymers can demonstrate some positive properties like biodegradability and biocompatibility that make them attractive implantation materials. The hydrolytic degradation of the polylactides result in random hydrolysis of their ester bonds. Any by-products that arise during the degradation of the polymers do not have any negative influence on the human body.

The lactic acid produced by the degradation of polylactic acid (PLA), because of their ester bonds being hydrolysed, is removed from the body via the citrate cycle. The following by-products being produced are water (H_2O) and carbon dioxide (CO_2) which are eliminated through the lungs. Another advantage is the malleability of the synthetic polymers, which allows them to be shaped into a wide variety of forms. This is based on their thermoplastic properties.

However, as seen in the Figure 3 above, polymers present also inconsiderable disadvantage such as a lower mechanical strength in comparison with Mg, other metals as well as ceramics. More precisely, the mechanical strength is reduced about half that of Mg. Thus, polymers are predominantly used in areas such as soft tissue reconstructions (20, 22, 25-29).

Advantages	Disadvantages	Clinical applications
□ High tensile strength	□ Rapid degradation:	□ Suture anchors
□ Excellent fibre-forming ability	– loss of mechanical strength	□ Meniscus repair
	– undesired inflammatory response	□ Interference screws
		□ Screws in fracture fixation

Figure 3: Biodegradable polymers and its benefits and disadvantages (22)

1.1.4 Metals

Metals are frequently used materials in medical fields and especially in areas such as load bearing applications where their excellent mechanical strength and fracture resistance are required.

Stainless steel (SS), titanium (Ti) and its alloys as well as cobalt-chromium (CoCr) alloys are conventional metallic implantation materials which, in addition to their positive properties as mentioned above, are also are accused of causing following disadvantages:

- In case of load bearing application, a so-called stress-shielding effect may occur because the metals (SS, Ti, CoCr) have much higher elastic modus compared to the bone.

  Thus, when loads are applied after insertion of the implant, the metallic implant takes much greater share of the load and the surrounding bone is less stressed. This stress shielding increased bone resorption around the implant.
- The corrosion of metals results in the release of metal ions which can introduce an inflammatory response.

In recent decades, various bioresorbable metallic implantation materials such as magnesium (Mg), zinc (Zn) and iron (Fe) have been developed (22, 25).

The properties that make Fe an interesting bioresorbable metal include high ductility and a high elasticity mode. The slow degradation rate of Fe can be increased by alloying it with, as an example, manganese (Mn). Zn is a non-toxic element which occurs physiologically in the human body while playing an important role in the immune system. The material properties of pure zinc include low rigidity and plasticity but also the capability to inhibit corrosion which is why Zn is used as an alloying element.

Mg has several properties that make it a very good bioresorbable material (Figure 4). These include excellent biocompatibility, osteoconductivity by promoting osteoclast activity, density and elastic modus similar to that bone and therefore preventing the occurrence of the stress shielding effect.

One reported disadvantage of high pure Mg is the high corrosion rate. Therefore, to reduce the corrosion rate, some alloying system as well as changes and

modifications of the Mg implants surface were developed and discussed in several existing studies.

Mg corrodes in the physiological environment by releasing species such as Mg^{2+} ions, alloying elements, hydrogen gas (H_2) and ions (OH^-). In the case of a particularly high accumulation and release of H_2 gas in the surrounding tissue, this can lead to a delay in bone healing and following decrease in implant stability or even loss of the inserted device (1, 2, 13, 20, 30).

Advantages	Disadvantages	Clinical application
□ Density similar to bone □ Good fracture toughness □ Elastic modulus similar to bone □ Readily degradable	□ Rapid degradation: – loss of mechanical strength – formation of H_2 gas bubbles delaying fracture healing	□ Screws in fracture fixation

Figure 4: Biodegradable Mg and its benefits and disadvantages (22)

1.2 Magnesium and its advantages

Magnesium is known as one of the lightest structural metals especially in terms of the density, which is 1.74 g/cm $^{-3}$ at 20°C. Whereas the density of the bone is approximately 1.9 g/cm $^{-3}$ and thus a similarly high density is present. It counts among the most abundant elements and is the eighth most abundant element in the outer layer of the Earth.

The human body is supplied with the bioactive trace element Mg partly intracellularly bound to chelators such as adenosine triphosphate (ATP) or adenosine diphosphate (ADP), and partly extracellularly and thus mainly via the blood.

Since the concentration of serum Mg is very well regulated, changes in homeostasis mostly affect extracellular Mg. The extracellular Mg, also called serum Mg, accounts for about 1% of the total balance of occurrence in the human body. As shown in the following figure 5 the extracellular Mg can be found bound to proteins, ionized as well as complexed (25, 31-34).

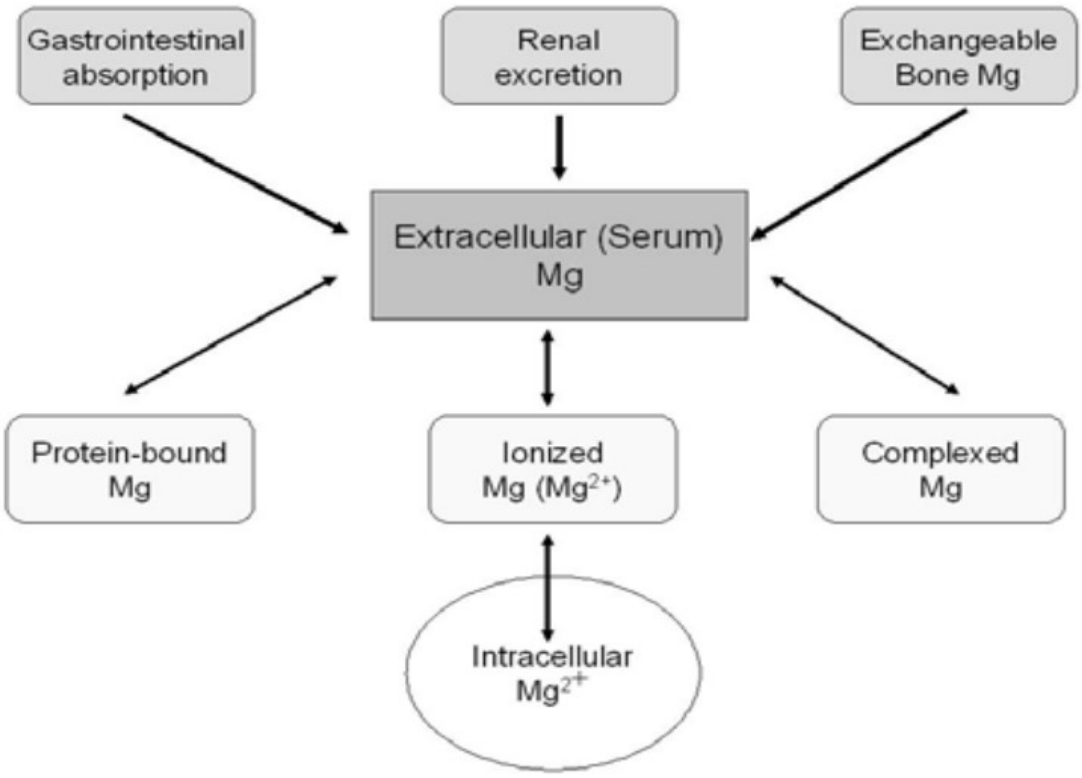

Figure 5: Illustration of the different systems regulating the balance of Mg located in the human body (31)

It is known that Mg is implicated in hundreds of enzymatic reactions in the human body (35, 36). Especially in those reactions regarding transfer, bearing and usage of energy.

The regulation of the Mg balance in the human organism is influenced by various complex mechanisms. These include for example storage in the bones (Figure 6), where more than 50% of the Mg in the human body is gathered and absorption via the digestive organs, especially via the jejunum and ileum.

The excretion of Mg present in the body occurs via renal excretion and so the control of Mg homeostasis is controlled via the kidneys. Hypomagnesemia and thus a Mg deficiency correlates with a decrease in bone density (2, 31, 37, 38).

Percent distribution	Concentration
Bone (60–65%)	0.5% of bone ash
Muscle (27%)	6–10 mmol/kg wet weight
Other cells (6–7%)	6–10 mmol/kg wet weight
Extracellular (<1%)	
Erythrocytes	2.5 mmol/l
Serum	0.7–1.1 mol/l
55% free	
13% complexes with citrate, phosphate, etc.,	
32% bound, primarily to albumin	
Mononuclear blood cells	2.3–3.5 fmol/cell
Cerebrospinal fluid	1.25 mmol/l
55% free	
45% complexed	
Sweat	0.3 mmol/l (in hot environment)
Secretions	0.3–0.7 mmol/l

Total body magnesium: 20–28 g (modified according to Shils, 1997).

Figure 6: Average percentage occurrence of Mg in the body if a healthy adult (32)

Due to its distinguished compatibilities such as a bone resembling density and elastic modulus as well as an outstanding biocompatibility and osseointegration, it has become established to use Mg as a biodegradable medical implant and therefore a possible alternative to conventional durable implant materials in different fields of medicine. Due to the elastic modulus similar to bone, the so-called stress shielding effect can be minimised, which would lead to the negative effect of resorption of the bone tissue according to the Wolff's law. Wolff's law means that bone is able to optimise its own structure in terms of density under changing loads so that it can continue to perform its maximum function. Mg mechanical strength

which provides respectively minimizes the stress shielding effect leads to the fact that they find usage in load bearing applications (39-41).

1.2.1 Degradation of Magnesium

The degradation of Mg and its alloys occurs in an aqueous environment due to the electrochemical reaction that is induced.
This reaction of Mg with water in aqueous solution leads to the formation of $Mg(OH)_2$, i.e. magnesium hydroxide as well as the formation of H_2 gas. $Mg(OH)_2$ as an insoluble product forms a kind of protective layer or barrier on the entire surface of the implant which protects against a too rapid corrosion reaction.
However, due to the binding to chloride ions if a concentration above 30mmol/L is prevailed, the Mg dissolves from the passive protective layer and the soluble magnesium chloride ($MgCl_2$) is formed. This can be transported further and excreted from the body. According to the literature by Song et al., the tolerable limit of the H_2 gas formed is an average formation of 0.01 mL/cm^2 per day (20, 42, 43).

The presence of chloride ions in the surrounding tissue influences the speed of degradation. Due to the constant exchange of chloride ions between the circulating blood and the surrounding tissue, a steady equilibrium of chloride ion concentration cannot be achieved, and degradation takes place until the implant is completely degraded (44).
Another factor that influences degradation is the pH value. An alkaline pH, i.e. >11.5, promotes the formation of the protective hydroxide layer and thus prevents too rapid degradation. In comparison, the pH value found in the *in vivo* environment, i.e. pH<11.5, accelerates degradation. Thus, in summary, a high chloride ion concentration in the surrounding tissue as well as a pH value < 11.5 lead to an unstable hydroxide layer associated with a fast corrosion rate on the implant surface (37, 44).

A therefore not inconsiderable problem that has been shown with the use of resorbable Mg implants is the rapid rate of degradation that may occur. This leads not only to the development and increased release of exactly this just mentioned H_2

but also consequently to the formation of cavities around the placed implant which subsequently leads to a loss of implant stability (45, 46).

As H_2 is a corrosion product of Mg in aquatic environments, it can be assumed that hydrogen is predominant in these cavities circularly around the implant (47).

It is known from numerous *in vitro* and *in vivo* studies that the degradation of Mg is not only influenced by the pH value and the concentration of chloride ions but also further various factors such as the temperature of the environment but also the composition of the alloy used (Figure 7). Slowing and reducing the corrosion rate of Mg, and thus reducing the formation of H_2, can be achieved by adding various biocompatible alloying elements such as Al, Zn, Mn, Zr and Ca.

Another way to reduce the degradation rate, is for example adding rare earth elements (REE) to those Mg alloys compostition. Representatives include elements such as Yttrium (Y) or Gadolinium (Gd).

However those REE are not physiologically present in the human body and must be cited that the occurrence of apoptosis and necrosis has been demonstrated with the use of Mg-alloyed implants containing those rare earth elements (2, 4, 48-50).

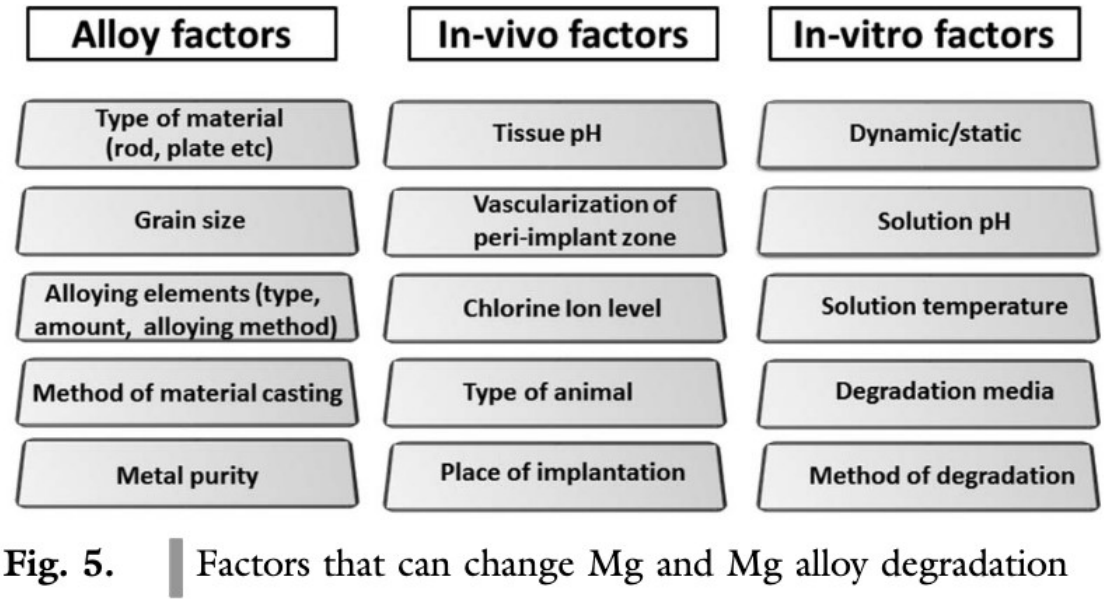

Figure 7: List of factors influencing the degradation behaviour of Mg and its alloys (1, 44)

1.3 Magnesium alloys

Magnesium and its alloys are suitable for use in medicine not only because of their excellent biocompatibility and properties such as the elastic modulus similar to those of bone but also because of their great mechanical possessions.
Thus, the elastic modulus of the human bone is about 40 to 57 GPa, while pure Mg has a modulus of elasticity of 45 GPa.
Mg is considered one of the most abundant bioactive trace elements in the human body and its ability to promote osteoclast activity can stimulate bone formation, growth and healing. This osteoconductive property leads to improved osseointegration of implants inserted. Another advantage in the use of Mg and its alloys is the fact that there is no need for a second operation to remove the implantation material from the healed insertion point and therefore avoiding possible comorbidities (2, 6, 42, 51-53). Within the last years, several *in vitro* as well as *in vivo* investigations have been reported, in which Mg alloys with different chemical compositions were tested (54).

A restriction or limitation with regard to clinical applications is the rate of degradation, which is associated with loss of structural integrity if it progresses too fast. It is therefore desirable that the rate of degradation of the Mg alloys tone with the rate of healing of the bone and thus is not too rapidly (45, 49, 55-57).

1.3.1 Pure Magnesium

The degradation rate of high-purity (HP) Mg (99.99%) has been reported between 10,5-210 mm per year (58). When looking at the differences in the rate of degradation between HP Mg and other Mg alloys, the former seems to have a much slower degradation. This can be due to the low contamination of HP Mg by impurifying elements such as Fe, Ni or Co. Low contamination is when the concentration of the contaminating elements remains below the tolerance limit of the respective element. In order to prevent a strong acceleration of the degradation and thus to achieve a good corrosion resistance, it is important not to exceed the

tolerance limits of the impurities. This means that a purification of the Mg alloys to achieve the desired slowing down of the degradation can be reached by adding pure Mg (59-62).

1.3.2 ZX00

Alloy ZX00 (MgZnCa; <0.5 wt.% Zn and <0.5 wt.% Ca) is a composition of Mg with calcium (Ca) and zinc (Zn).

Ca has a low density of 1.55 g/cm^3, occurs physiologically in human bones and plays an important role in cellular signal transmission. By adding Ca to the alloy compositions, a positive effect on bone healing can be achieved. The proportion of Ca should not exceed a concentration of 1%.

Zn is an significant representative of the trace elements found in the human body and is essential for immunological function and metabolism. If it is added to an alloy, this increases the tolerance to impurities from other elements and consequently leads to an increase in corrosion resistance. The addition of Zn also reduces H_2 gas evolution. Cai et al. were able to demonstrate an increase in mechanical strength and corrosion resistance with a Zn content of up to 5 wt.% (2, 63-66).

1.4 Titanium and it’s alloys

The metal titanium has the atomic number 22 in the periodic table of the elements and thus belongs to the transition metals. It also has a very low density of only 4.5g/cm and is silver in colour. The melting point of this metal is 1668° Celsius (67, 68).

The use of Ti and its alloys as well as other metals such as stainless steel (SS) or alloys based on cobalt- chromium (CoCr) has been practiced in medicine for decades. This is because of this element's excellent biocompatibility, minimal toxicity, enhanced resistance against corrosion and exceptional mechanical and elastic properties. Due to these possessions, Ti has become a commonly used material and is still considered the gold standard in the selection of implantation materials in different medical fields and particularly in dentistry. It is found both in endosseous dental implants as well as in prosthetic restorative materials.
The application of Ti as well as other metallic materials can be found mainly in areas where a property of particularly high fracture toughness is required. Ti is therefore primarily used in load bearing applications (4, 25, 69, 70).

Another property that should be mentioned is the ability to form a direct bond with the tissue of the bone. This can be explained by the presence of a thin oxide layer that forms on the surface of the titanium with a thickness of approximately 1.5-10 nanometer. This oxide layer is formed when the metal is exposed to air or water during manufacturing and production.
The emerged passive oxide layer is responsible for the ability to achieve a good osseointegration. In addition, it also provides a good corrosion resistance as this layer prevents too much electron flow between the implant and the peri-implant tissue (71-73).

Different mechanical properties between bone and Ti materials have been noticed especially regarding fracture toughness and mechanical strength. Ti has in comparison to Mg a modulus of elasticity not comparable to that of bone.
Due to the stiffness of this metal and its alloys, that is almost twice as high as that of the bone, the stress shielding effect may emerge.

This is due to the altered loading of the bone that occurs during Ti implant placement. When this so-called stress shielding effect occurs, the load that the implant must bear is much higher than that of the surrounding bone tissue.
According to Wolff's law, the bone reacts to stress as it comes to remodelling and this on the other hand leads to resorption of the surrounding bone tissue, resulting in reduced stimulation of bone growth and impaired implant stability.
In the field of orthopedics, especially in case of high bearing loading, this stress shielding can lead to revision surgery and explantation of the implants placed with a possible risk of potential comorbidities. From a radiological point of view, this phenomenon is determined as radiolucent areas (50, 68, 74-76).

Regarding the use of titanium in the field of oral implantology, no proven long-term clinical damage has been recorded to date. Nevertheless, possible negative effects in the surrounding tissue and thus on the human body due to the absorption of titanium ions in body fluids, for example, are critically discussed in the literature (25, 77).

1.4.1 Pure titanium (cp-Ti)

Pure titanium or also called commercially titanium is classified in 4 different degrees of purity, which are characterized by the different contents of oxygen (O), carbon (C) and iron (Fe).
Grade 1 means that the lowest level of impurities with carbon, oxygen and iron is present. As the oxygen content increases, the strength increases, and the toughness properties are minimized.
It should be mentioned that the Ti implants used in dentistry mostly have a purity grade of 4, as this has a particular strength (12, 78-80).

1.4.2 Ti-6Al-4V

Modification with regard to the phase composition of titanium and thus also changes in properties can be achieved by the addition of different alloying elements such as aluminium (Al), iron (Fe), silver (Ag) or vanadium (V) (68).

Ti-6Al-4V also known as Grade V titanium is one of the most commonly used titanium alloys in medicine. In orthopaedics, for example, as fixation screws for bone fractures, but also in dentistry as a conventional material for implants, pins and for prosthetic superstructures like crowns and bridges. This alloy is constituted as follows: 6 wt% aluminium and 4 wt% vanadium (81, 82).

However, the use of this alloy potentially releasing vanadium and aluminium ions, can lead to health consequences such as an allergic reaction up to severe physical damages like peripheral neuropathy or Alzheimer diseases. Some studies reported toxic effects on the body when implants of this alloy are left in place for a longer period of time (68, 83, 84).

1.5 Galvanic corrosion

Galvanic corrosion happens when two unlike metals with different electrochemical potentials, such as Ti and Mg, meet in the presence of an electrolyte which offers them a path for the transfer of electrons (e^-) (25, 67, 85). The result is a transfer of electrons from the anode to the nobler metal, the cathode (Figure 8). This causes corrosion and therefore the release of undesirable corrosion by-products of the anode (25, 86, 87).

Mg occupies the place of the most reactive metal in the entire electrochemical series with an electrochemical potential of -2.37 V and thus represents the most active metal in galvanic series, which causes it to become anodic in any corrosion reaction. In contrast, Ti has an electrochemical potential of -1.63 V and has therefore an electrochemical potential similar to that of Mg. In order to keep the corrosion rate as low as possible, it makes sense to use metals such as Mg and Ti for co-implantation, as they have very similar electrochemical potentials (25, 88).

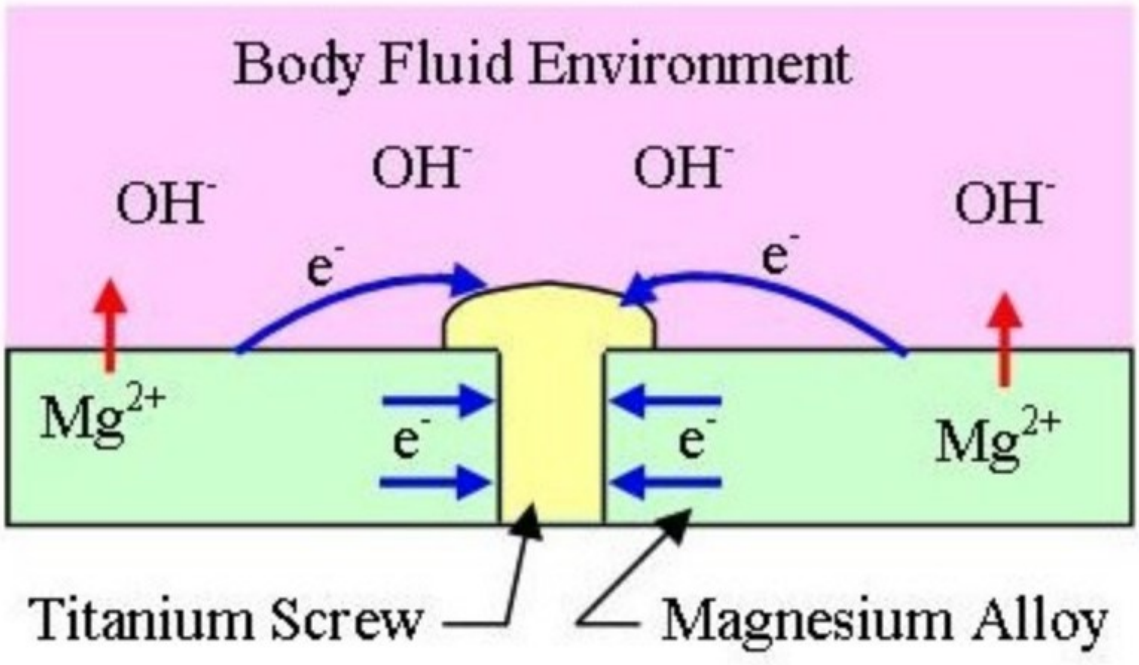

Figure 8: Illustration of a galvanic reaction between metals (Ti and Mg) of different electrochemical potentials (25)

In their publication, Song and Atrens define the process of corrosion as *"all physical and chemical features and processes involved when metallic magnesium is exposed to an environment"* (89).

Considering the corrosion reactions of biodegradable metals such as Mg alloys, anodic dissolution as well as cathodic reduction reaction occurs under physiological conditions. Immediately after the biodegradable Mg has contact with a body fluid such as saliva, it acts as an anode and an anodic reaction occurs as shown in Equation 1 (90-92).

Equation 1:

$$M \rightarrow M^{n+} + ne^{-}$$

In Equation 2, electrons generated in this reaction are consumed to reduce water. This process corresponds to a cathodic reaction. These anodic and cathodic reactions take place on the entire surface of the inserted implant.
Physiological conditions such as the presence of proteins or chloride or hydroxide ions, as well as dissolved oxygen, provide a corrosive environment for Mg (90-92).

Equation 2:

$$2H_2O + 2e^{-} \rightarrow H_2 + 2OH^{-}$$

Equation 3 shows the hydroxide layer formed on the entire surface of the Mg. This layer can be considered as a kinetic barrier and prevents further chemical reactions from occurring on the surface. However, the presence of chloride ions can result in an even more rapid degradation of this passive protective layer (50, 90-92).

Equation 3:

$$M^{n+} + nOH^{-} \rightarrow M(OH)_n$$

In general, the corrosion behaviour of metals and their alloys is determined by the potential of the aqueous environment. These potentials are not constant values but can change depending on the type and composition of the electrolytes. Thus, the corrosion rate is also influenced by the existing pH value in the surrounding tissue and its fluctuations (25, 67).

Also, due to the chloride ion concentration in the human body fluid, the related corrosion rate increase. Not only water, proteins and dissolved oxygen are found in human body fluids. But also, a number of chloride and hydroxyl ions which, as mentioned above, leads to the development of a corrosive environment for the Mg.

Due to the negative electrochemical potential of Mg, metal ions begin to migrate from the surface of the metal into the surrounding fluid. These ions in turn begin to form species capable of forming an oxide layer on the surface of the metal.

This layer adheres to the entire surface of the metal and serves as a passive protective layer. As a result, further migration of free ions on the metal surface can be prevented.

Corrosion is also always associated with the formation of H_2 as a corrosion by-product, which spreads or accumulates in a circular manner around the implant in the bone tissue and leads to a formation of subcutaneous gas bubbles.

As a result, alkalinisation of the solution or local alkalization in the area of the implant can occur and consequently an imbalance of the pH-dependent reaction equilibrium (25, 42, 92, 93).

In order to reduce the corrosion rate of Mg alloys, besides the possible change in alloy composition different implant modification methods are used. These can be changes of the implant surface properties by for example laser peening or modifications of the surface by coating of single, double or multiple layers of for example HA or polymers but also by the application of chemical processes (50, 94-96).

2 Hypothesis and aim of this study

In the field of oral implantology, two types of implants are used clinically: (i) semi-permanently implant to restore the shape and function of the defect site, usually composed of titanium, (ii) those placed temporarily for instance bioresorbable bone fixation materials. In the last decades, Mg and its alloys have shown to be a bioresorbable alternative to conventional implant material due to their excellent biocompatibility, mechanical properties, biodegradability and osteoconductivity. Because of their opposite potential in the galvanic series, Mg and Ti are subject to galvanic corrosion which can affect their mutual influence on material properties and degradation rates.

The aim of this study is to investigate *in vivo* the corrosion kinetics between co-implanted durable (Ti) and bioresorbable (Mg) material, and to evaluate their mutual influence on material properties and degradation rates.

In summary, the following assumptions were made:

i. *Because of their opposite potential in the galvanic series, we expect that Mg-based implants will degrade faster in presence of Ti.*
ii. *Moreover, we hypothesize that the distance (5 mm or 10 mm) between the two different materials will influence the degradation of Mg-based implants.*

This animal experiment involved transcortical co-implantation of titanium (Ti-6Al-4V) and magnesium (ZX00) pins made with Mg-0.45 Zn-0.45 Ca in wt% to test the above-mentioned hypotheses.

In order to be able to quantify the mutual influence of the materials with regard to degradation, formation of H_2 gas on each other, the rats were randomly divided into four different groups.

In the first group (group 1), Ti and ZX00 pins were co-implanted with a distance of 5 mm, for the second group (group 2) Ti and ZX00 pins were co-implanted with a distance of 10 mm. There were also two control groups in which the ZX00 pins were separated by a sham spaced by 5 mm (group 3) and 10 mm (group 4).

3 Material and methods

3.1 Ethical statement

Small animal experiments were approved by the Austrian Federal Ministry of Science and Research and followed the guidelines for the accommodation and care of animals formulated in the European Convention for the Protection of Vertebrate Animals used for Experimental and other Scientific Purposes.
In accordance with the 3R principles (replace, reduce and refine), all animal experiments were conducted in a way that minimised animal suffering. The experimental animals had an acclimatisation period of 7 days after arrival until the start of the experiment.

3.2 Materials

The Mg-based alloy, ZX00 (Mg-0.45 Zn-0.45 Ca in wt%), was used in this study. This material was co-implanted with turned Ti-6Al-4V (Titanium grade 5). Pins (Ø= 1.4 mm, h = 6 mm) were used for this *in vivo* study. After production, the samples were packaged and sterilized by gamma radiation dose.

3.3 Method

3.3.1 Experimental design

Twenty-four male Spraque Dawley® rats (n=24) at the age of 4 weeks (body wt 120-140 g) were randomly assigned to four experimental groups.
The animals were housed in a conventional facility with a day/night cycle of 12 hours each. Permanent access to food and water was also provided for the entire study.

As above mentioned, the rats were divided into 4 groups of 6 rats per each group. The transcortical implantation of the pins was performed in both the right and left diaphysis of the tibia of each rat. In Table 1, the group distribution of the test animals is explained as follows:

In the first group, the transcortical co-implantation of the ZX00 pin with the Ti pin was carried out at a distance of 5 mm from each other.

In group 2, however, the implantation of the same materials took place with a distance of 10 mm.

In group 3, a ZX00 pin and a sham were implanted transcortical at a distance of 5 mm from each other.

In group 4, a sham was implanted with a distance of 10 mm to the ZX00 pin.

Group 1	ZX00 co-implanted with titanium with a spacing of 5 mm
Group 2	ZX00 co-implanted with titanium with a spacing of 10 mm
Group 3	ZX00 without titanium with a spacing of 5 mm
Group 4	ZX00 without titanium with a spacing of 10 mm

Table 1: experimental design groups

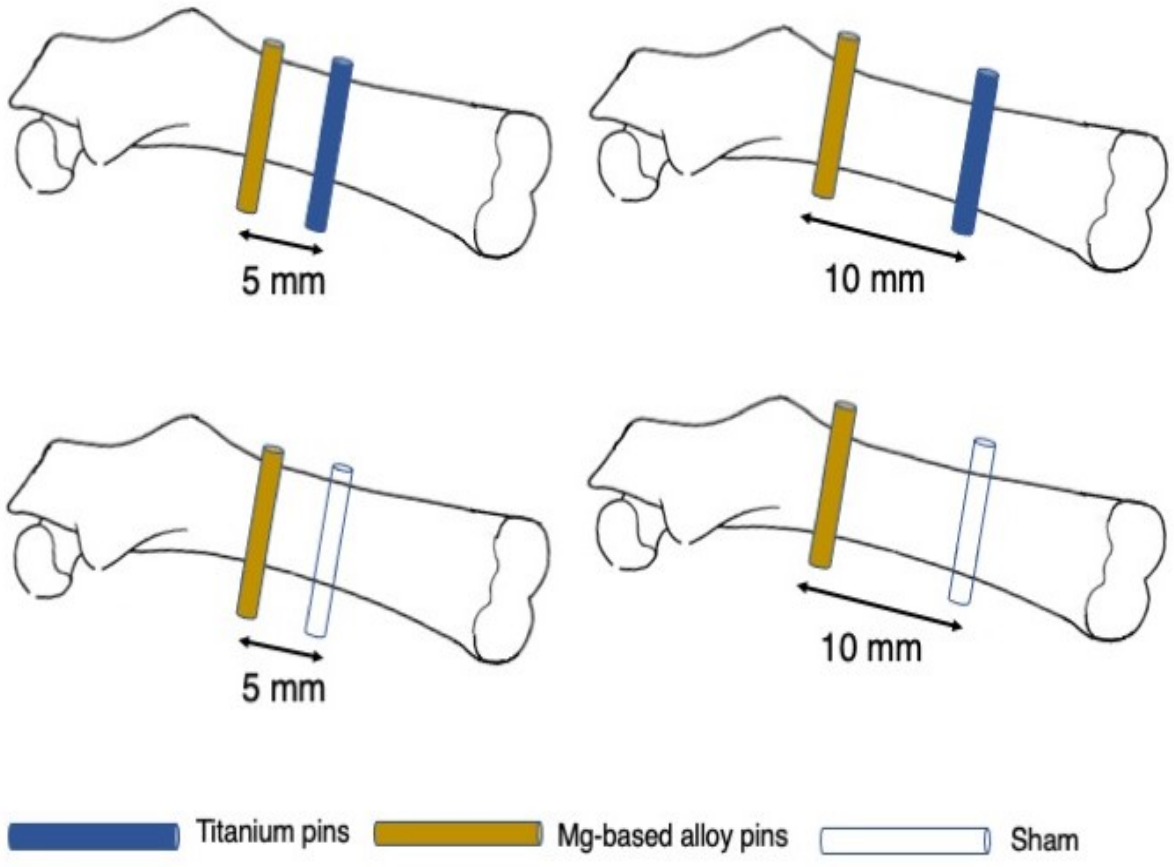

Figure 9: Illustration of the experimental design using the example of a femur

On the top left, experimental group 1 with the co-implantation of ZX00 with Ti with a distance of 5 mm. On the top right, experimental group 2 with co-implantation of ZX00 with Ti at a distance of 10 mm. At the bottom left and right, experimental groups 3 and 4, and thus control groups, are shown with implantation of ZX00 at a distance of 5 mm and 10 mm with a Sham

Six randomly chosen rats per group (i.e. twelve femora) were investigated by µCT evaluation at prearranged time points. The implementation took place on the day of the implantation as well as 4-, 8- and 12- weeks post-implantation. Which results in a total observation period of 12 weeks. The rats were subsequently sacrificed at week 12 as well as they were subjected to histological analysis at week 12 post implantation.

3.3.2 Surgical procedure

Both the implantation of the pins and all following examinations were performed under general anaesthesia. The anaesthesia is given by 0.1 ml/100 g bodyweight (bw) FDD anaesthetic solution subcutaneous (s.c.) (Table 2) and is antagonized with 0.1 ml/100 g bw antidote solution intraperitoneally (i.p.). (Table 3)
Postoperatively, after assured awakening, the rats are returned to the animal house. Immediate postoperative pain therapy is given by 0.4 ml s.c. administration, and for 1 week postoperatively via drinking water. (Table 4 and 5)
Under anaesthesia, the fur was shaved over the entire tibia of the rat. The shaved area was sterilely washed with Betadine solution.
A skin incision of approximately 1 cm length was made in the already disinfected left and right area of the tibia.
The cortical bone is then dissected free, sparing the musculature, and then on the tibial diaphysis, two parallel transcortical implantation beds with a diameter of 1.6 mm and a spacing of either 5 or 10 mm were pre-drilled individually.
In the group 3, however, only one transcortical implantation bed was pre-drilled in the diaphysis of the rats tibia.
In the groups in which a co-implantation of magnesium and titanium was planned, the Mg-alloy pins were implanted at the distal part of the tibia and the Ti-pins will be implanted at the proximal part. To avoid thermical necrosis of the bone tissue, the drilling was performed under constant irrigation with physiological saline solution.
The cylindrical implant was then inserted into the newly created drill channel and the wound was subsequently closed in layers with a resorbable suture with Vicryl rapid 4-0 single button sutures.

Medicament	**Active ingredient**
1 ml Fentanyl	50 µg Fentanyl
1 ml Dormicum	1 mg Dormicum
0,5 ml Domitor	0,5 mg Medetomidin

Table 2: composition antidote solution

Medicament	Active ingredient
4 ml Anexate	0,4 mg Flumazenil
0,5 ml Antisedan	2,5 mg Atipamezol
1,5 ml NaCl	

Table 3: postoperative pain medication s.c.

Medicament	Active ingredient
1 ml Rimadyl	50 mg Carprofen
50 ml NaCl	

Table 4: postoperative pain medication (drinking water)

Medicament	Active ingredient
4 ml Dipidolor	15 mg Piritramid
20 ml Glucose 5%	
250 ml water	

Table 5: composition FDD anesthetic solution

3.3.3 Euthanasia

For euthanasia, volatile Isoflurane was deployed for sedative anaesthesia of the animals. Followed by subsequently injection of 25 mg sodium thiopental (Thiopental® Sandoz, Sandoz GmbH, Kundl, Austria) into the cardiac ventricle which led to immediate cardiac arrest.

In the next step, the tibiae of rats were extracted, and all soft tissues were carefully removed. The bone implant specimens of ZX00 alloy was subsequently fixed in neutral buffered formalin solution and further processed for the following histological examination.

3.3.4 Microfocus Computed Tomography (µCT)

In vivo µCT (Siemens Inveon µCT device) scans at a resolution of 35µm were performed at previously defined time points: immediate after implantation, 4, 8 and 12 weeks after implantation.
During the Microfocus computed tomography the animals were anesthetized with volatile isoflurane.
The micro-CTs performed made it possible to observe parameters to be examined such as the rate of degradation and pin surface of the ZX00 pins *in vivo*, tibia lengths and to determine the subsequent adaptation of the bone tissue.
After the scans were performed, the implanted pins and bubbles of emitted H_2 were reconstructed as 3D models by using the image processing software MIMICS, version 23.0 (Materialise Mimics). Afterwards a quantification of the pin volume (mm^3), pin surface (mm^2), tibia lengths (mm) and gas volume (mm^3) could be performed.

3.3.5 Evaluation of implant degradation parameters of the ZX00 pins

In order to obtain a precise quantification of the degradation behaviour of the implants including implant volume, surface and gas volume, each tibia of the 24 rats was considered individually.
For this purpose, the "Image - Reslice-Images" function was used to display the implant in all three planes and in all layers in such a way that an exact assessment was possible. The evaluation was carried out using MIMICS software, version 23.0 (Materialise Mimics).

3.3.6 Evaluation of degradation and implant surface of the ZX00 pins

For the three-dimensional (3D) representation of the implants, a mask was first placed on the images. This was done by activating the tool "Segment - New Mask".

For this, a threshold value for the Hounsfield (HU) units, which was approximately 220-3000, was specified.

Since the bone and the placed ZX00 implants have similar HU units, which in turn makes it difficult to differentiate the implant surface from the bone, the threshold units were reworked by an individual adjustment. By separating the µCT images using the "Segment - Split Mask" tool, an accurate representation of the implants could be achieved by colouring the bone red and the ZX00 pin blue (Figure 10, b.). This function also required manual post-processing of each slice in the axial, longitudinal and coronal planes to achieve an exact representation of the implants. Lastly, the tool "Mask - Calculate part" was selected to obtain a 3D representation of the implant. Then a quantitative analysis of the implant surface (mm^2) and the implant volume (mm^3) could be carried out.

a.

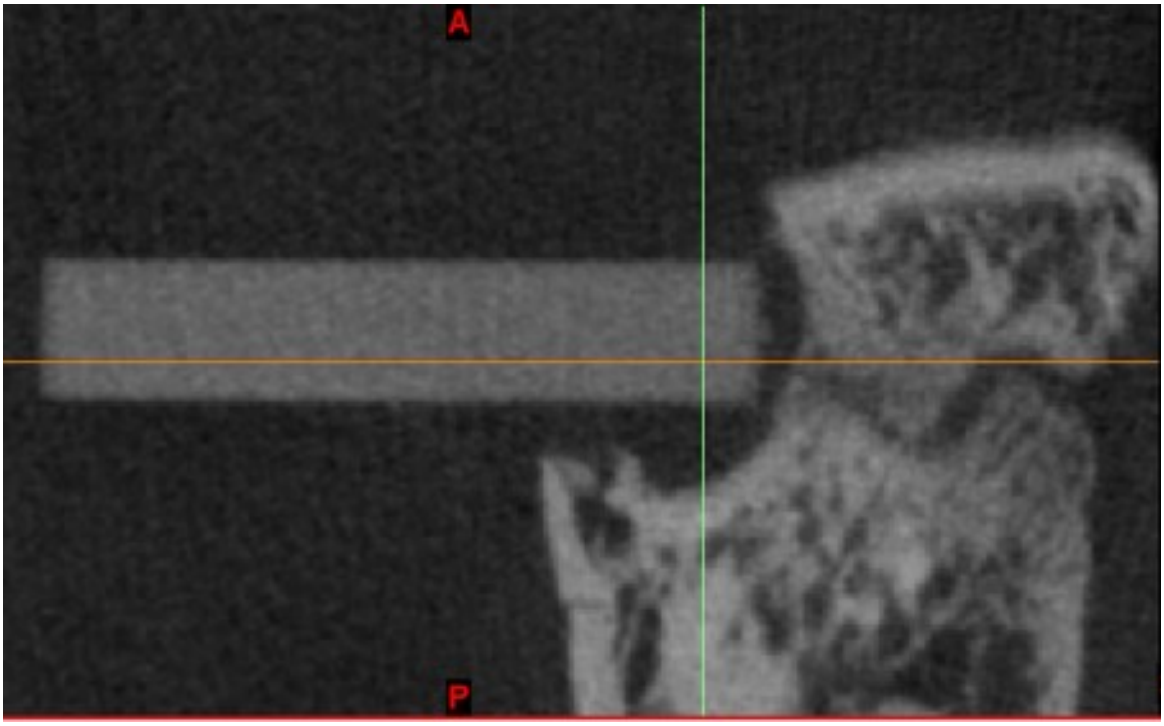

b.

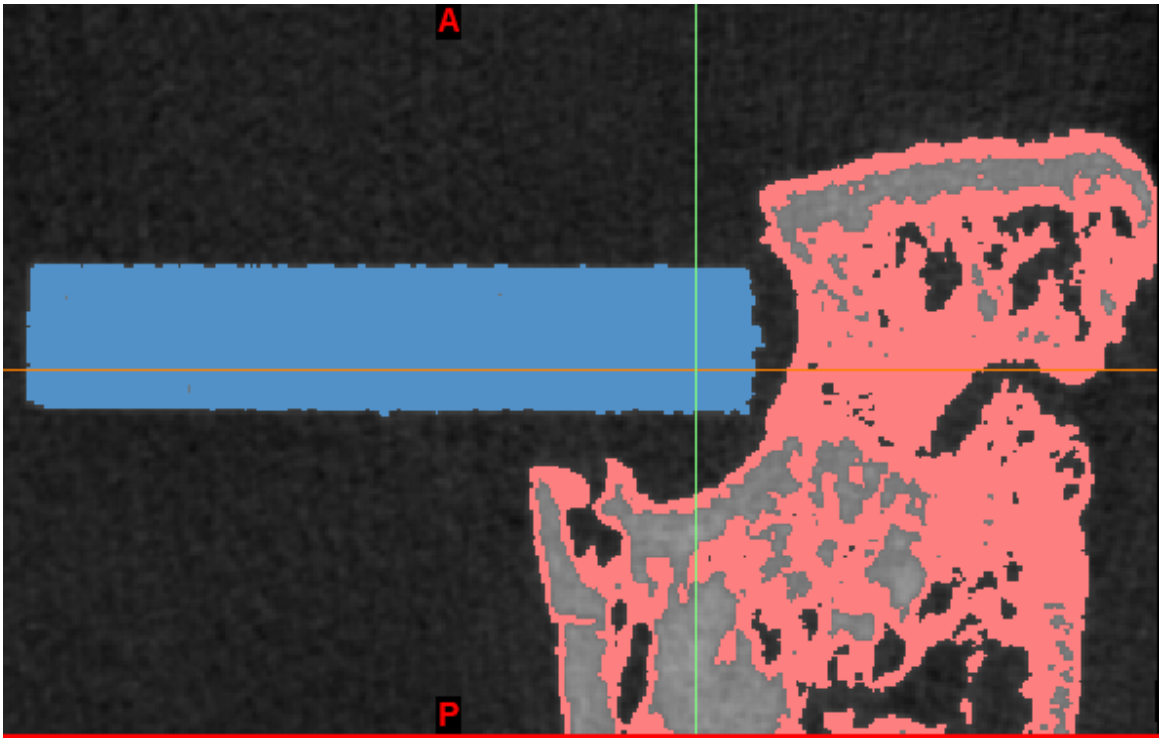

c.

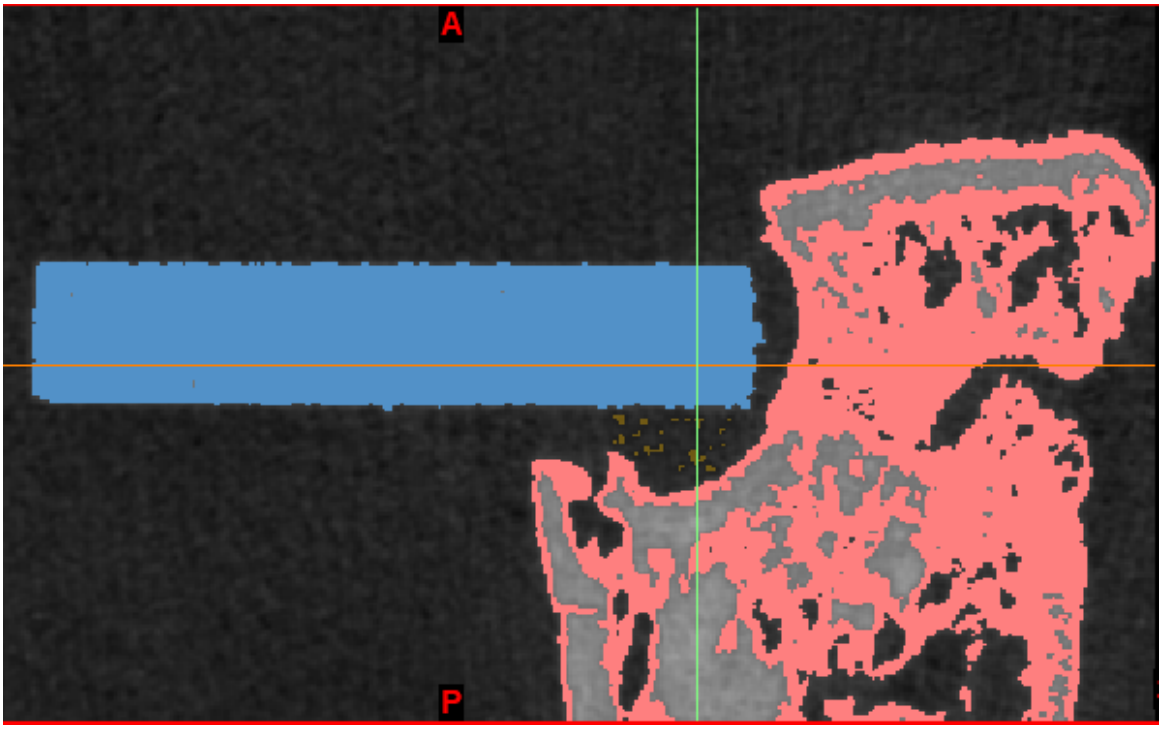

Figure 10: µCT images

For the analysis of the parameters implant surface, implant volume and hydrogen gas volume, µCT images (a.,b. and c.) were acquired at the defined time points T 0, W 4, W 8 as well as W 12 and analysed and quantified with the software MIMICS, version 23.0. Representation of the proximal tibia bone including an inserted ZX00 pin (a.). In order to

distinguish the bone (red) from the ZX00 pin (blue) and thus quantify the parameters to be examined, the function "Segment - Split Mask" was activated in the MIMICS software, version 23.0 (b.). With the help of "Mask - Split Mask" the emitted peri-implant H_2 gas bubbles are made identifiable (c.).

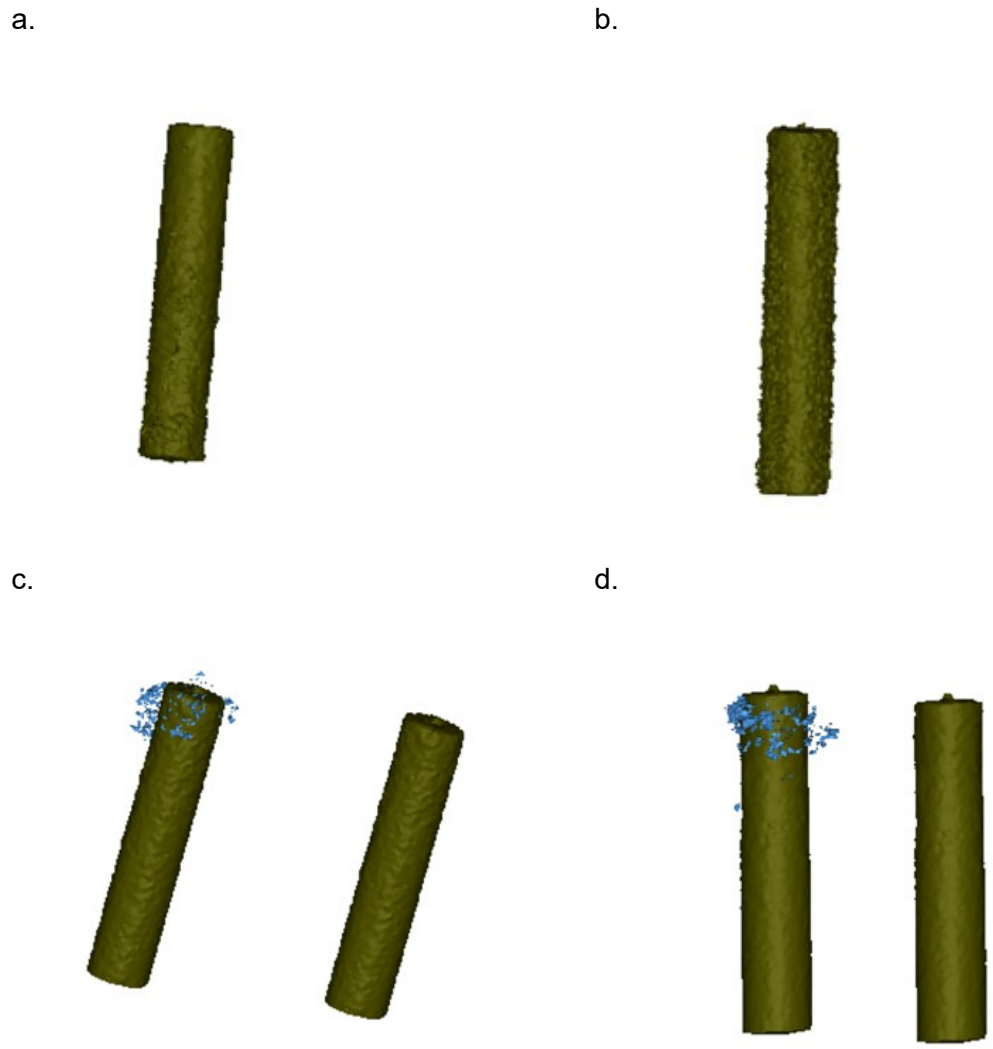

Figure 11: 3D reconstructed ZX00 pins via Mimics software, version 23.0

Three-dimensional representation of the surface of the ZX00 implants using the MIMICS software, version 23.0 (Materialise Mimics) to quantify the implant volume (mm^3) as well as the implant surface (mm^2) and gas volume (mm^3) using the example of the left tibia (9051_left) at the time points T 0 (a.), W 4 (b.), W 8 (c.) and W 12 (d.).

3.3.7 Evaluation of the H_2 gas volume of the ZX00 pins

Another mask was activated by the “Segment – New mask” tool. For this purpose, the threshold values of the HU units were defined in advance with -1000 to -1050, although an individual adaption of these was also required at this point.
In the next step, a 3D model of the H_2 gas was created using the tool “Mask – Calculate part” and then the volume of the evolved gas was calculated in mm^3.

3.3.8 Evaluation of the Tibia length

The evaluation of the measuring tibia length is done by marking the eminentia intercondylaris as well as the lowest point of the facies articularis at the tibiae and measuring the distance between our measuring points by selecting the function "Measure - Length" at all time points (T 0, W 4, W 8 and W 12).

3.3.9 Histological test

In order to be able to perform the histological examination, the tissue blocks which contained the implants were fixed in neutral buffered formalin solution, dehydrated in ascending grades of alcohol and embedded in light-curing resin.
For processing the samples, we used Technovit® 9100 which is a low temperature Methyl methacrylate (MMA) embedding system.
After polymerization, those specimens got cut through the central axis of the implant as well as parallel to the longitudinal axis of the tibial shaft.
150µm thin sections were prepared using a microtome saw with a diamond blade.
The produced ground sections were stained with methylene blue and basic fuchsine. Qualitative histological evaluation has been carried out by to use of a light microscope.

3.3.10 Statistical analysis

The parameters of our study's data were assessed, reported as means ± standard deviations (SD), and their means were compared using an ANOVA.
P-values of less than 0.05 (<0.05) were considered significant for the statistical analysis, which was conducted on the material ZX00 at the indicated time points T 0, W 4, W 8, and W 12.

4 Results

The Sprague-Dawley® rats, randomly divided into four groups (groups 1-4) of six animals each, underwent a transcortical implantation of the pins in the right and left tibia.
The six animals in group 1 underwent transcortical co-implantation of the Mg-pins (ZX00) and Ti pins at spaced by 5 mm. In group 2, the same implantation took place, but with a distance of 10 mm.
In group 3, which served as the control group, the animals were implanted with ZX00-pins and sham-pins at a distance of 5 mm.
In group 4, which also served as a control, the sham was co-implanted with the ZX00-pin at a distance of 10 mm.

In vivo µCT was performed at predetermined time points. These time points were directly on the day of implantation (T 0) and at week 4 (W 4), 8 (W 8) and 12 (W 12) post-implantation. Using these µCT images, the parameters to be investigated for our study, such as ZX00 implant volume, gas volume, implant surface and tibia length, could be determined.

4.1 Magnesium implant volume

In order to quantify the degradation behaviour of the implanted ZX00 pins, the µCT scans performed *in vivo* at the time points T 0, W 4, W 8 and W 12 were visualised with the image processing software MIMICS, version 23.0.
Based on the scans performed at the different time points, the changes in the volumes of the Mg pins and thus the degradation behaviour was evaluated.

The mean initial volume of the Mg pins (ZX00) at T 0, i.e. on the day of implantation, was 16.79 mm^3 ± 0.77 mm^3 standard deviation (SD) in group 1. After four weeks, a slightly smaller volume was recorded with an average value of 15.90 mm^3 ± 0.59 mm^3. Thus, there was a slight increase in volume to a value of 16.42 mm^3 ± 0.88 mm^3 in week eight after implantation. Another decrease in the mean volume to 14.89 mm^3 ± 0.88 of the ZX00 pins was recorded in week twelve.

In group 2, the mean initial volume of the Mg pins was 15.92 mm^3 ± 0.38 mm^3 at baseline (T 0). In terms of initial pin volume, there was a small increase in volume to 16.59 mm^3 ± 0.52 mm^3 by week 4 (W 4). By week eight, there was already a slight decrease in volume to 16.44 mm^3 ± 1.99 mm^3. Twelve weeks after implantation, the mean pin volume decreased to 14.76 mm^3 ± 1.51 mm^3.

The mean initial volume (T 0) of ZX00 pins in group 3 was calculated with an average value of 16.00 mm^3 ± 0.81 mm^3. Four weeks after implantation (W 4), a small change in volume was observed at 16.07 mm^3 ± 0.73 mm^3.
After eight weeks (W 8), a small decrease in pin volume to 16.03 mm^3 ± 5.11 mm^3 was recorded. After twelve weeks, the pins had a mean volume of 14.15 mm^3 ± 0.41 mm^3. Thus, there was a decrease in relation to the initial volume (T 0).

In group 4, the mean ZX00 pin volume was 16.39 mm^3 ± 0.84 mm^3 directly after implantation. In week four (W 4), the mean volume was 16.12 mm^3 ± 0.57 mm^3 and thus showed a slight mean reduction. A reduction in volume from T 0 to T 4 could therefore also be quantified in this group. Eight weeks after implantation, a mean volume of 15.50 mm^3 ± 0.81 mm^3 was recorded. After twelve weeks, the mean

volume of 14.78 mm^3 ± 0.82 mm^3 showed a significant reduction compared to the initial pin volume.

ZX00 implant volume (mm^3)								
	Group 1		Group 2		Group 3		Group 4	
	Mean	SD	Mean	SD	Mean	SD	Mean	SD
T 0	16,798	0,774	15,922	0,384	16,001	0,810	16,392	0,840
W 4	15,907	0,591	16,586	0,525	16,074	0,729	16,117	0,567
W 8	16,425	0,876	16,437	1,987	16,033	5,113	15,498	0,806
W 12	14,895	0,876	14,756	1,509	14,150	0,413	14,784	0,820

Table 6: descriptive statistics of the measured implant volumes (mm^3) of the ZX00 pins at the specified examination times

In all groups (groups 1-4), a small reduction in the mean initial pin volume (T 0) was observed up to week four.

From week four (W 4) to week eight (W 8), with the exception of group 1 where there was a minimal increase in volume, there was a small decrease regarding the mean age ZX00 pin volume in groups 2-4.

After twelve weeks, the mean volume of the ZX00 pins decreased in all four groups compared to the initial volumes observed.

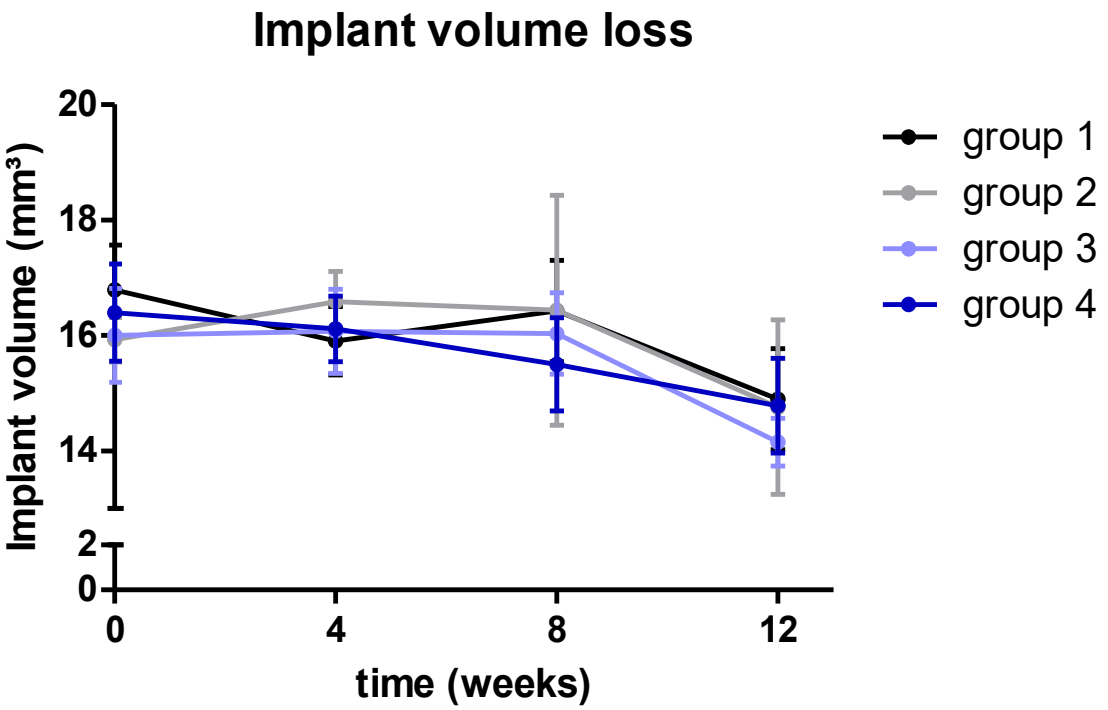

Figure 12: Alteration in implant volume loss

Demonstration of the development of the values (mm^3) of the ZX00 implant volume at the time points T 0, W 4, W 8 and W 12. Shown as mean value ± standard deviation (SD).

4.2 Gas volume

In order to measure the hydrogen gas evolution associated with the degradation of the bioresorbable Mg pins, µCT scans were performed at T 0 (on the day of transcortical implantation), after four weeks (W 4), after eight weeks (W 8) and after twelve weeks (W 12).
The gas cavities that formed around the ZX00 pins were visualized by a three-dimensional reconstruction with the image processing program MIMICS, version 23.0 in order to quantify them.

At the time T 0, i.e. on the day of implantation, a mean gas volume of 0 mm^3 ± 0 mm^3 could be measured in all experimental groups (groups 1-4).

In group 1, a mean gas volume of 0.44 mm^3 ± 0.63 mm^3 was measured after four weeks (W 4). After eight weeks (W 8), the mean gas volume was 0.45 mm^3 ± 0.33 mm^3, which corresponds to a mean increase. In week twelve (W 12) the highest accumulation of H_2 could be measured with a mean of 1.18 mm^3 ± 0.26 mm^3.

In group 2, an increase in the mean gas volume from 0 mm^3 to 0.25 mm^3 ± 0.33 mm^3 was observed from the day of implantation to week four (W 4). In week eight (W 8), the mean H_2 volume increased to 0.35 mm^3 ± 0.26 mm^3.
The highest recorded volume was observed in week twelve (W 12) with a mean gas volume of 1.03 mm^3 ± 0.41 mm^3.

In the investigations of group 3, a mean H_2 volume from T 0 to week 4 (W 4) of 0.30 mm^3 ± 0.44 mm^3 was reported.
After eight weeks (W 8), a mean gas volume to 0.20 mm^3 ± 0.11 mm^3, which corresponds to a reduction was reported.
A renewed increase to 1.02 mm^3 ± 0.64 mm^3 took place by week twelve (W 12).

In experimental group 4, the mean gas volume increased from 0 mm^3 to 0.23 mm^3 ± 0.34 mm^3 by week four (W 4). A slight reduction of the mean recorded volume to 0.17 mm^3 ± 0.09 mm^3 could be observed until week eight (W 8), until finally in week twelve the highest mean volume with 1.02 mm^3 ± 1.29 mm^3 could be recorded.

Gas volume (mm^3)								
	Group 1		Group 2		Group 3		Group 4	
	Mean	SD	Mean	SD	Mean	SD	Mean	SD
T 0	0	0	0	0	0	0	0	0
W 4	0,437	0,631	0,251	0,333	0,301	0,441	0,227	0,343
W 8	0,452	0,335	0,352	0,258	0,197	0,115	0,172	0,088
W 12	1,183	0,264	1,026	0,415	1,021	0,643	1,022	1,292

Table 7: descriptive statistics of the measured gas volume (mm^3) of the ZX00 pins at the specified examination times

All groups started with an initial (T 0) gas volume of 0 mm^3 ± 0 mm^3. By week four (W 4), a slight increase was recorded in all groups, but group 1, and thus the group with co-implantation at 5 mm, recorded the highest H_2 gas development at 0.45 mm^3 ± 0.33 mm^3.

There was another slight increase in groups 1 and 2 up to week 8, but there was a decrease in the control groups (groups 3 and 4). Up to W 12, the volume of H_2 gas increased in all groups, with group 1 also recording the highest value with 1.18 mm^3 ± 0.26 mm^3.

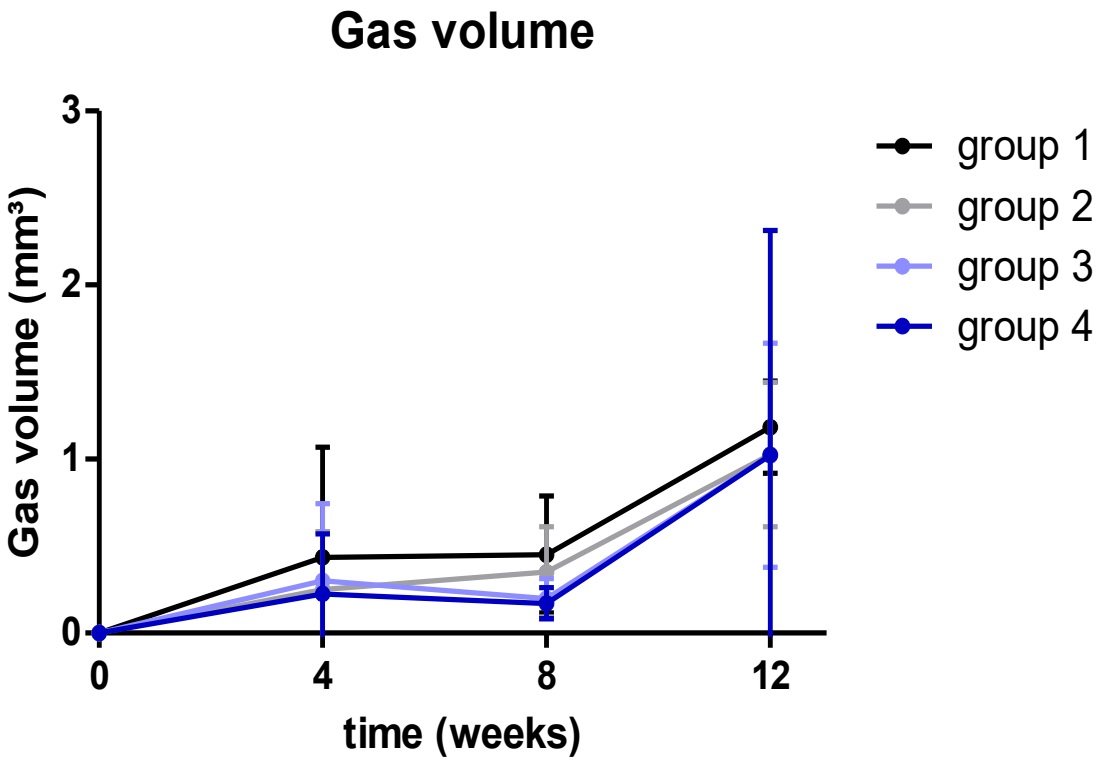

Figure 13: Alteration in gas evolution

Demonstration of the development of the values (mm^3) of gas volume at the time points T 0, W 4, W 8 and W 12. Shown as mean ± standard deviation (SD).

4.3 Magnesium implant surface

The changes on the surface of the ZX00 pins caused by degradation could be reconstructed and measured using the µCT scans at the time points T0, W 4, W 8 and W 12. The analysis of the scans was also carried out here using MIMICS, software, version 23.0.

At the beginning of the µCT examinations (T 0), the ZX00 pins in group 1 had a mean implant surface of 58.04 mm^2 ± 5.63 mm^2.
After four weeks (W 4), a mean surface area of 55.91 mm^2 ± 7.01 mm^2 was recorded, which corresponds to a reduction to the initial value.
By the last observation point in week twelve (W 12), the mean implant surface decreased to 45.12 mm^2 ± 1.39 mm^2.

In group 2, a mean implant surface of 52.73 mm^2 ± 4.33 mm^2 was observed at the beginning (T 0). Four weeks after implantation (W 4), only a slight implant surface decrease corresponding to 52.22 mm^2 ± 4.76 mm^2. By the next observation time after week eight (W 8), there was a mean increase of the implant surface to 54.93 mm^2 ± 4.54 mm^2. This was followed by a mean decrease to 43.90 mm^2 ± 2.09 mm^2 until the measurement in week twelve (W 12).
Accordingly, in this group there was a mean reduction over the entire study period.

In group 3, the initial (T 0) ZX00 surface was 51.84 mm^2 ± 4.58 mm^2. By week four (W 4), a reduction of the implant surface to 49.59 mm^2 ± 1.99 mm^2 could be recorded. A slight increase to 50.63 mm^2 ± 5.04 mm^2 by week eight (W 8) was recorded. At the last measurement point (week 12), the mean implant surface dropped again to an average of 45.17 mm^2 ± 1.44 mm^2. Thus, 12 weeks after implantation, there was a reduction in baseline values in all groups.

In group 4, the mean ZX00 implant surface was 54.79 mm^2 ± 4.93 mm^2 at the beginning of the measurements (T 0). In week four (W 4), a mean decrease to 51.49 mm^2 ± 4.20 mm^2 was reported. Followed by a slight reduction to 50.54 mm^2 ± 3.89 mm^2 up to week eight (W 8).

Twelve weeks after implantation (W 12), the mean implant surface was 44.89 mm^2 ± 3.39 mm^2. In general, there was an average reduction from T 0 to W 12 when comparing the initial values with the final values.

ZX00 implant surface (mm^2)								
	Group 1		Group 2		Group 3		Group 4	
	Mean	SD	Mean	SD	Mean	SD	Mean	SD
T 0	58,044	5,629	52,73	4,326	51,840	4,578	54,786	4,930
W 4	55,914	7,015	52,221	4,760	49,589	1,990	51,491	4,200
W 8	50,525	2,937	54,935	4,543	50,628	5,041	50,537	3,895
W 12	45,125	1,386	43,902	2,095	45,17	1,443	44,886	3,387

Table 8: descriptive statistics of the measured implant surface (mm^2) of the ZX00 pins at the specified examination times

As seen in Table 8, the highest initial mean implant surface (T 0) was measured in the group 1 with 58.04 mm^2 ± 5.63 mm^2.

Between T 0 and W 4, a reduction of the mean implant surface took place in all groups (1-4). After 4 weeks, there was a statistical difference in term of implant surface regarding the group 1 in comparison with the other groups.

In week four, a decrease in the values was already recorded in all groups, whereby the highest value of 55.91 mm^2 ± 7.01 mm^2 was still measurable in group 1.

There was a decrease regarding the mean implant surface in the groups 1 and 4 after eight weeks (W 8). In contrast, an increase was recorded in group 2 and 3.

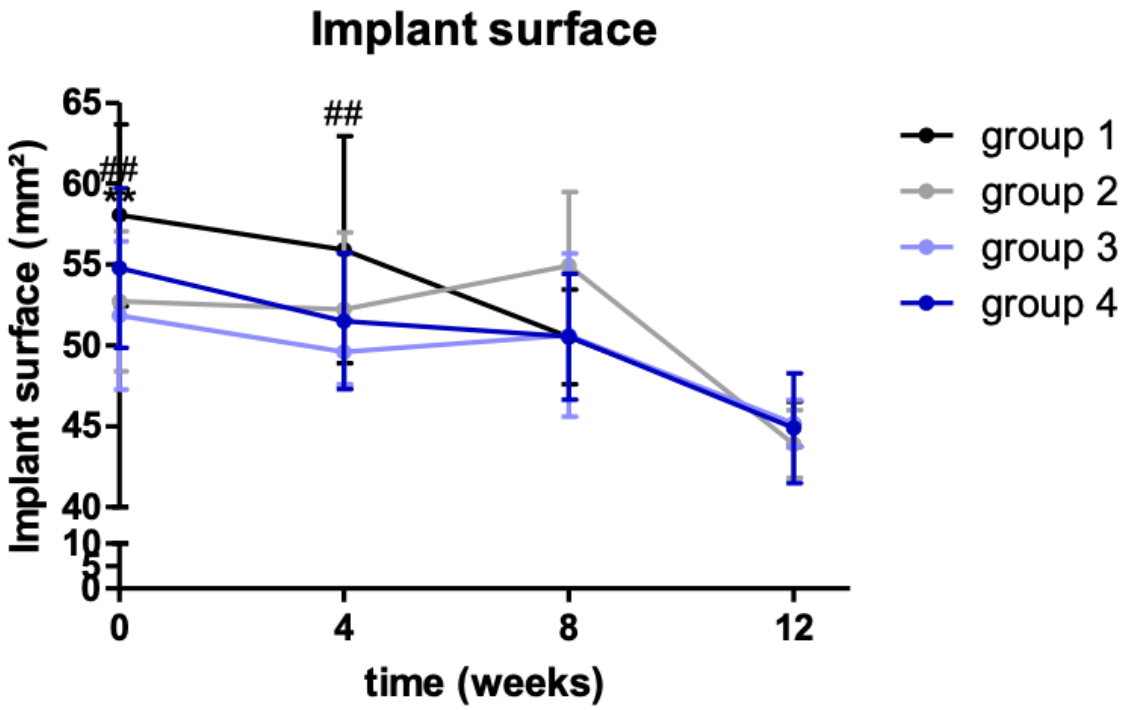

Figure 14: Alteration in implant surface

Demonstration of the change in the values (mm^2) of the ZX00 implant surfaces at time points T 0, W 4, W 8 and W 12. Shown as mean ± standard deviation (SD).

4.4 Tibia length

Another parameter that was also observed in the µCT evaluations was the tibial length.

In order to be able to make a statement about whether transcortical co-implantation in the diaphyseal area influences longitudinal bone growth and thus leads to restrictions in terms of growth. Especially if the implantation takes place in relative proximity to the growth plate of the bone. The evaluation of the tibial lengths, more precisely the longitudinal bone growth, was performed by µCT at the examination times T 0, W 4, W 8 and W 12 and could be visualised with the image processing software MIMICS, Version 23.0.

In all groups, an increase in the length of the measured bones was observed between the individual measurement times (T 0, W 4, W 8 and W 12) and thus no restriction of longitudinal growth could be found.

Tibia length (mm)								
	Group 1		Group 2		Group 3		Group 4	
	Mean	SD	Mean	SD	Mean	SD	Mean	SD
T 0	27,166	0,921	27,35	0,470	27,525	0,609	27,391	0,932
W 4	31,95	1,131	32,39	0,452	32,381	0,821	32,363	0,852
W 8	34,94	2,090	35,625	1,182	35,444	1,314	35,5	1,337
W 12	35,3	1,681	36,562	0,914	36,781	1,465	37,145	1,564

Table 9: Descriptive statistics of the measured tibia lengths (mm) at the specified examination times

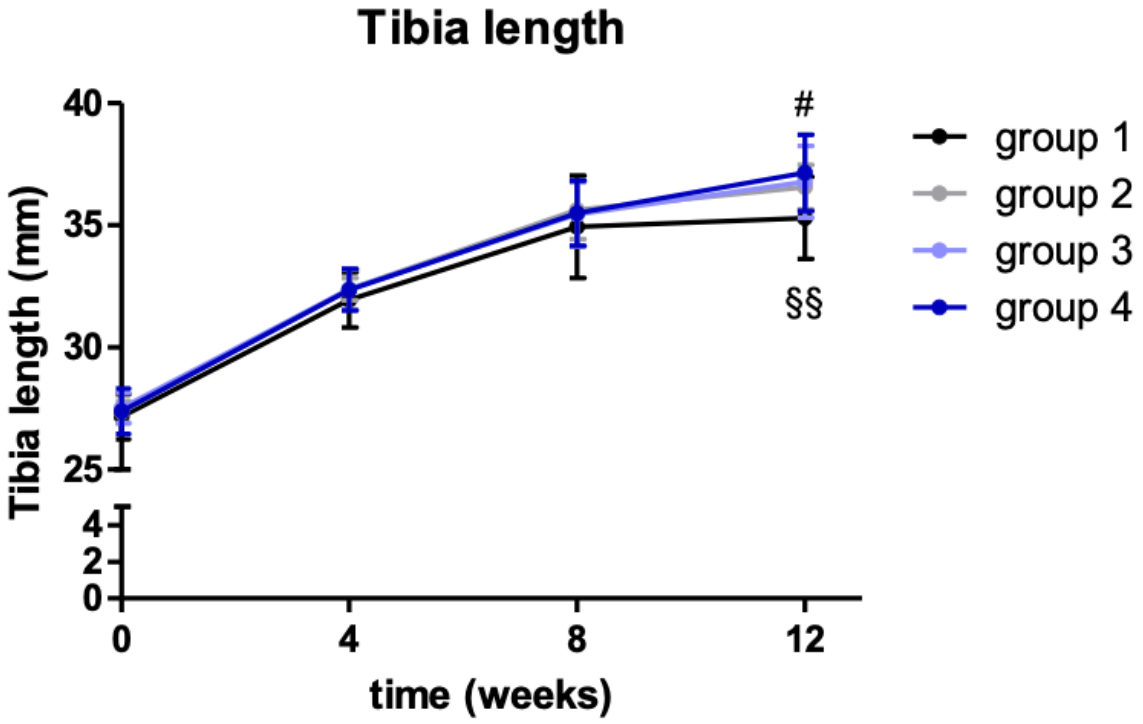

Figure 15: Evolution of the tibial length during time

Representation of the increase in length of the left and right tibiae (mm), and thus longitudinal bone growth of the test animals at the time points T 0, W 4, W 8 and W 12. Data is shown as mean ± SD.

4.5 Histological evaluation

For the qualitative histological examination, tissue blocks containing the implants were removed from the experimental animals after euthanasia, i.e. twelve weeks after implantation. After fixation of these tissue samples in neutral buffered formalin solution and embedding in light-curing resin, they were stained with basic fuchsin and methylene blue for descriptive analysis. The Technovit® 9100 (Kulzer GmbH, 63450 Hanau, Germany) embedding system was used for this purpose. The histological examination was then carried out using a light microscope. The tissues that appear blue are soft tissue, while bone can be identified by the pink staining. Since older bone appears dark pink, it can be easily distinguished from newly formed bone tissue, which appears light pink.

Based on histological evaluation, homogeneous degradation of ZX00 pins was observed. H_2 gas cavities appear circularly around the implants and are partly separated by bone.
Osteoclast activity as well as newly formed bone, which can be recognised by its light pink colour, was detected in all groups (group 1-4). Due to the newly formed bone, the occurrence of direct bone-implant contact (BIC) is seen. Furthermore, no signs of infection could be detected.

a.

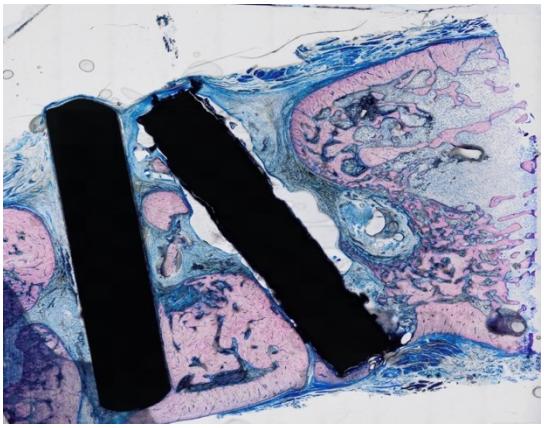

b.

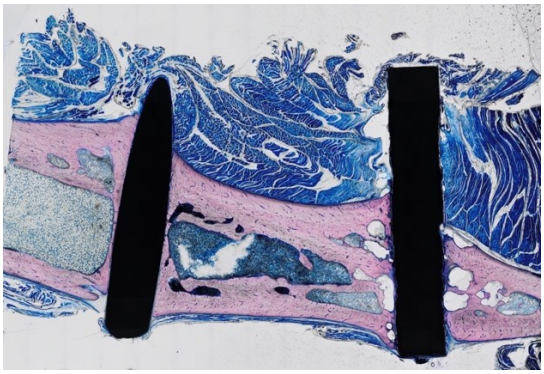

c.

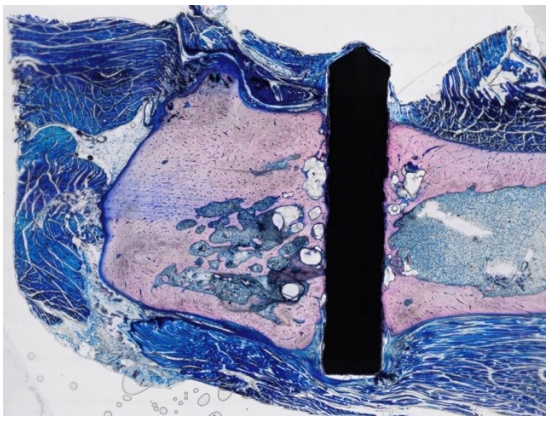

d.

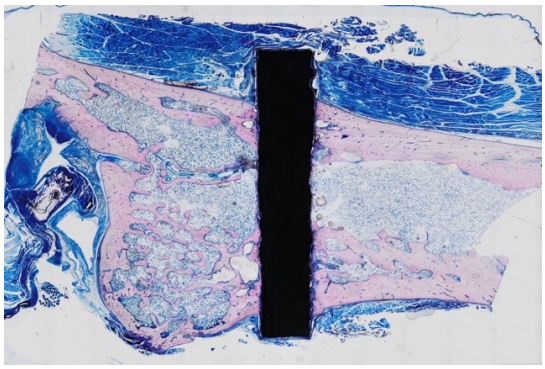

Figure 16: Histological slides

Qualitative histology using a Laczko Levai staining of a tibia: co-implantation of ZX00 with Ti with a space of 5 mm (a.) and 1 0mm (c.) and a spacing of ZX00 with a sham by 5 mm (b.) and 10 mm (d.).

5 Discussion

Materials used in dental implantology can be classified into ceramics, polymers and metals due to their different chemical background (13).

Despite the positive properties of ceramics and polymers, the use of metallic implantation materials such as Ti and its alloys is currently the gold standard. Titanium is used mainly because of its excellent mechanical properties, low toxicity, good biocompatibility and, above all, its corrosion resistance, which is achieved by the formation of a thin oxide layer on the implants surface that prevents excessive electron flow between the implant and the peri-implant tissue (13, 20, 85). Despite the remarkable advantages of using titanium in dental surgery, orthopaedics and traumatology, it is worth considering the use of bioresorbable alternatives. The use of biodegradable materials can avoid the need for a second operation to surgically remove a permanent Ti implant and therefore may avoid the occurrence of possible intra- and postoperative risks. It must also be considered that after successful bony integration or healing of the titanium implants, metal ions can be successively released into the surrounding tissue, and thus potential long-term damage can occur (44, 54).

To be considered as a suitable implantation material, certain requirements must generally be fulfilled regarding material properties. These include an excellent biocompatibility, good mechanical properties, high corrosion resistance, ductility and good osseointegration of the material. However, biocompatibility depends on the corrosion resistance of the material. Thus, if corrosion progresses too fast, corrosion products such as metal ions are released into the surrounding tissue and can potentially cause damages (97-100). Mg fulfils the required material properties and thus appears to be a good bioresorbable alternative to conventional implantation materials. In addition, Mg has an elasticity mode similar to bone, which minimises the risk of the occurrence of the so-called stress shielding effect which would lead to a reduced bone-growth stimulation and therefore loss in implant stability. Due to the natural occurrence of Mg as a trace element in the human body, it does not cause inflammatory or rejection reactions and thus has excellent biocompatibility (4, 101). Since the 20th century, using Mg as an implantation material has gained interest, which is why there are already several studies on this

topic (1, 4, 9, 102, 103). For example, a recent study by Kačarević et al. investigated the use of pins made of the Mg alloy WZM211 to fix membranes in case of guided bone regeneration (GBR). Adequate fixation of the membrane in the critical early healing phase was achieved, preventing epithelial and connective tissue healing of the bony defect. Furthermore, a complete gradually progressive resorption could be observed up to week 52 (104).
Co-implantation of Mg and another biomedical metal such as Ti can result in changes of the corrosion behaviour of the bioresorbable Mg. As Mg is known to be the most reactive metal in the galvanic series and therefore always acts as an anode with the other metal reacting as a cathode. This leads to an increased corrosion rate. Considering the study of Hou et al. where a transcortical co-implantation of high-purity Mg with Ti screws into the femora of SD rats at a distance of 5 and 10 mm took place, an acceleration of corrosion was already observed after eight weeks. According to their hypothesis, the accelerated corrosion was due to the formation of a galvanic like cell by the inserted HP Mg and Ti screws through the existing blood vessels in the periosteum (3, 25, 85).

In our study, pins made of a Mg alloy (ZX00) were implanted transcortically in the diaphysis of the tibiae of the SD rats together with pins made of Ti-6Al-4V. As a control, two of the experimental groups (groups 3 and 4) were implanted with ZX00 pins without Ti. *In vivo* micro-computed tomography scans with a resolution of 35µm were performed at the specified time points: 0, 4 and 8 weeks after surgery. After euthanasia of the animals, thus 12 weeks after implantation, *ex vivo* µCT scans with a resolution of 15µm were performed and samples were taken for a qualitative histological analysis. To quantify the implant volume, implant surface and gas volume, a 3D reconstruction of the µCT images was performed using MIMICS software, version 23.0 (Materialise, Louvain, Belgium).

If we look at the average implant volume at the defined examination times, no significant differences between the four test groups could be observed. However, 4 weeks after implant placement, a statistical difference regarding the implant surface was reported in the group 1 in comparison to the other groups. This can be attributed to the formation of an oxide layer on the implant surfaces. According to Witte et al., the degradation of Mg alloy materials leads to the formation of corrosion products

such as Mg hydroxides and Mg oxides, which in turn lead to the formation of this corrosion layer. The formation of this layer is assumed to slow down the progress of corrosion and thus achieve successful osseointegration (105).

If we look at the study by Hou et al., in which HP Mg pins were co-implanted with Ti pins at a distance of 5 mm (group MT 5) and 10 mm (group MT 10) into the diaphyses of SD rats femur, a stronger volume and hence faster corrosion was found in the group in which HP Mg was co-implanted with Ti at a distance of 5 mm. In this study, it is also assumed that the distance between the pins affects the degradation rate.
Furthermore, it is hypothesised that due to abundant blood vessels in the area of the insertion site of this study, i.e. the periosteum and endosteum, the formation of a galvanic-like cell takes place, and this leads to faster corrosion. This is due to the fact that electrons can bind to proteins in the blood plasma and thus the electron transport from the anode (Mg) to the cathode (Ti) can take place (3).
It can already be seen from other studies that there are differences in the degradation rates and their speed in relation to the different implantation sites. For example, there is more perfusion in the epiphyseal areas than in the metaphyseal and diaphyseal areas of the bone, which leads to more rapid degradation due to the rapid disappearance of degradation by-products (101, 106). In the study by Kraus et al. in which they investigated the degradation of ZX00 and WZ21 pins, the fastest degradation progress was quantified in the soft tissue area, which they attributed to the good blood supply and the stability of the local pH value, which is subject to only a small fluctuation range (107).

There was a moderate decrease in implant surface from the beginning in all groups and over the entire study period. Again, during time no significant differences were found between the groups with the different insertion distances of 5 and 10 mm between ZX00 and Ti and the groups 3 and 4 with the sham insertion. This indicates that there was no noticeable difference of degradation rate by increasing the distance between the ZX00 and Ti pins.

The *in vivo* degradation of Mg and its alloys in an aqueous environment such as body fluid is based on the following corrosion reaction: $Mg + 2H_2O \rightarrow Mg(OH_2) +$

H_2. The resulting magnesium hydroxide ($Mg(OH)_2$) leads to the formation of an insoluble protective layer on the metal surface and thus prevents further corrosion. At a local chloride ion concentration of >30 mmol/l, the magnesium ions start to bind to chloride ions which leads to the formation of the soluble magnesium chloride ($MgCl_2$). $MgCl_2$ can then be excreted from the human body. When saturation of the peri-implant tissue as well as the blood with hydrogen is reached, diffusion into the surrounding tissue can no longer occur. Consequently, the accumulation of H_2 gas in the tissue cavities occur (1, 20, 62, 105, 108). In our study, the group with co-implantation of ZX00 with Ti of 5 mm showed a slightly stronger H_2 gas development at all time points compared to the other test groups, but this difference was not statistically significant.

No comparable studies could be elicited, so no comparison on H_2 gas development was possible. There are, however, already some material science studies that deal with the degradation properties and thus also with the H_2 gas evolution of Mg alloys. Due to the increasing interest in the use of bioresorbable implantation materials, further experiments on potential co-implantation with alternative materials would be relevant. It would be useful to expand the duration of the study until the complete degradation of the Mg pins in order to quantify the extent of the gas evolution. Furthermore, this would allow a better observation of the healing process of the bony defects.

Considering the study by Kraus et al. in which ZX50 pins were implanted in the diaphyses of the femora of rates, no damage to the peri-implant tissue was recorded and a restitutio ad integrum of the bony defect was achieved despite strong H_2 development due to the rapid degradation (107).

Regarding the tibia length, in all groups an increase in the length of the measured bone was observed between the individual measurement times (T 0, W 4, W 8 and W 12). Therefore, no restriction of longitudinal growth could be found in this study. This fact indicates also the possible use of Mg-based devices for children with growing bones.

Overall, the results of our study showed a homogeneous degradation of the ZX00 pins without significant differences regarding the distance to the co-implanted Ti pins. A physiological increase in tibial length was also observed in all groups,

suggesting that longitudinal bone growth was not affected. Further investigations are needed to determine the positive effect of new bone formation induced by the Ca precipitated on the implant surface as described in the literature (1).

A limitation for the clinical application of resorbable Mg and its alloys is the complex process of degradation in case of co-implantation. In order to establish itself as a safe alternative to already existing and above all, clinically proven biometals, it is necessary to study the galvanic corrosion between Mg and Ti in more in details.

6 Conclusion

In the study, we observed a homogenous degradation of the ZX00 pins, which was also accompanied by an acceptable hydrogen gas evolution.
No significant differences were observed between the different experimental groups, especially regarding the distance between the co-implanted ZX00 and titanium pins.
Nevertheless, further *in vivo* and clinical investigations are required including the entire degradation period of bioresorbable Mg to obtain more precise information on the gas evolution and its influence on the peri-implant tissue.

7 References

1. Pogorielov M, Husak E, Solodivnik A, Zhdanov S. Magnesium-based biodegradable alloys: Degradation, application, and alloying elements. Interventional Medicine and Applied Science Interventional Medicine and Applied Science. 2017;9(1):27-38.

2. Herber V, Okutan B, Antonoglou G, N GS, Payer M. Bioresorbable Magnesium-Based Alloys as Novel Biomaterials in Oral Bone Regeneration: General Review and Clinical Perspectives. J Clin Med. 2021;10(9).

3. Hou P, Han P, Zhao C, Wu H, Ni J, Zhang S, et al. Accelerating Corrosion of Pure Magnesium Co-implanted with Titanium in Vivo. Scientific Reports. 2017;7(1):41924.

4. Staiger MP, Pietak AM, Huadmai J, Dias G. Magnesium and its alloys as orthopedic biomaterials: A review. Biomaterials. 2006;27(9):1728-34.

5. Fischerauer SF, Kraus T, Wu X, Tangl S, Sorantin E, Hänzi AC, et al. In vivo degradation performance of micro-arc-oxidized magnesium implants: A micro-CT study in rats. Acta Biomaterialia. 2013;9(2):5411-20.

6. Esmaily M, Svensson JE, Fajardo S, Birbilis N, Frankel GS, Virtanen S, et al. Fundamentals and advances in magnesium alloy corrosion. Progress in Materials Science. 2017;89:92-193.

7. Negrescu AM, Necula M-G, Costache M, Cimpean A. In vitro and in vivo biological performance of Mg-based bone implants. Rev Biol Biomed Sci. 2020;3:11-41.

8. Planell JA, Navarro M. 1 - Challenges of bone repair. In: Planell JA, Best SM, Lacroix D, Merolli A, editors. Bone Repair Biomaterials: Woodhead Publishing; 2009. p. 3-24.

9. Afshar A, Steensma DP, Kyle RA. Albin Lambotte: Pioneer of Osteosynthesis (Bone Fixation). Mayo Clinic Proceedings. 2021;96(7):2012-3.

10. Witte F. The history of biodegradable magnesium implants: A review. Acta Biomaterialia. 2010;6(5):1680-92.

11. Morris AH, Kyriakides TR. Matricellular proteins and biomaterials. Matrix Biology. 2014;37:183-91.

12. Schenk RK, Buser D. Osseointegration: a reality. Periodontology 2000. 1998;17(1):22-35.

13. Binyamin G, Shafi BM, Mery CM. Biomaterials: A primer for surgeons. Seminars in Pediatric Surgery. 2006;15(4):276-83.

14. Zizzari VL, Zara S, Tetè G, Vinci R, Gherlone E, Cataldi A. Biologic and clinical aspects of integration of different bone substitutes in oral surgery: a literature review. Oral Surgery, Oral Medicine, Oral Pathology and Oral Radiology. 2016;122(4):392-402.

15. Campana V, Milano G, Pagano E, Barba M, Cicione C, Salonna G, et al. Bone substitutes in orthopaedic surgery: from basic science to clinical practice. Journal of Materials Science: Materials in Medicine. 2014;25(10):2445-61.

16. for the Committee on Biological I, Greenwald AS, Boden SD, Goldberg VM, Khan Y, Laurencin CT, et al. Bone-Graft Substitutes: Facts, Fictions, and Applications. JBJS. 2001;83(2).

17. Lee S-W, Kim S-G. Membranes for the Guided Bone Regeneration. Maxillofac Plast Reconstr Surg. 2014;36(6):239-46.

18. Wang J, Wang L, Zhou Z, Lai H, Xu P, Liao L, et al. Biodegradable Polymer Membranes Applied in Guided Bone/Tissue Regeneration: A Review. Polymers. 2016;8(4):115.

19. Sheikh Z, Qureshi J, Alshahrani AM, Nassar H, Ikeda Y, Glogauer M, et al. Collagen based barrier membranes for periodontal guided bone regeneration applications. Odontology. 2017;105(1):1-12.

20. Grün NG, Holweg PL, Donohue N, Klestil T, Weinberg A-M. Resorbable implants in pediatric fracture treatment. Innovative Surgical Sciences. 2018;3(2):119-25.

21. Sakamoto M, Matsumoto T. Development and evaluation of superporous ceramics bone tissue scaffold materials with triple pore structure a) hydroxyapatite, b) beta-tricalcium phosphate. Bone regeneration. 2012:301-20.

22. Godavitarne C, Robertson A, Peters J, Rogers B. Biodegradable materials. Orthopaedics and Trauma. 2017;31(5):316-20.

23. Nery EB, LeGeros RZ, Lynch KL, Lee K. Tissue Response to Biphasic Calcium Phosphate Ceramic With Different Ratios of HA/βTCP in Periodontal Osseous Defects. Journal of Periodontology. 1992;63(9):729-35.

24. Gauthier O, Bouler J-M, Aguado E, Pilet P, Daculsi G. Macroporous biphasic calcium phosphate ceramics: influence of macropore diameter and macroporosity percentage on bone ingrowth. Biomaterials. 1998;19(1):133-9.

25. Poinern GEJ, Brundavanam S, Fawcett D. Biomedical magnesium alloys: a review of material properties, surface modifications and potential as a biodegradable orthopaedic implant. American Journal of Biomedical Engineering. 2012;2(6):218-40.

26. Gunatillake PA, Adhikari R, Gadegaard N. Biodegradable synthetic polymers for tissue engineering. Eur Cell Mater. 2003;5(1):1-16.

27. Gentile P, Chiono V, Carmagnola I, Hatton PV. An Overview of Poly(lactic-co-glycolic) Acid (PLGA)-Based Biomaterials for Bone Tissue Engineering. International Journal of Molecular Sciences. 2014;15(3):3640-59.

28. Yan J, Li J, Runge MB, Dadsetan M, Chen Q, Lu L, et al. Cross-linking Characteristics and Mechanical Properties of an Injectable Biomaterial Composed of Polypropylene Fumarate and Polycaprolactone Co-polymer. Journal of Biomaterials Science, Polymer Edition. 2011;22(4-6):489-504.

29. Asgari M, Hang R, Wang C, Yu Z, Li Z, Xiao Y. Biodegradable Metallic Wires in Dental and Orthopedic Applications: A Review. Metals. 2018;8(4):212.

30. Lastra MD, Pastelin R, Camacho A, Monroy B, Aguilar A. Zinc intervention on macrophages and lymphocytes response. Journal of trace elements in medicine and biology. 2001;15(1):5-10.

31. Touyz RM. Magnesium in clinical medicine. Front Biosci. 2004;9:1278-93.

32. Vormann J. Magnesium: nutrition and metabolism. Molecular Aspects of Medicine. 2003;24(1):27-37.

33. Okuma T. Magnesium and bone strength. Nutrition. 2001;17(7):679-80.

34. Jahnen-Dechent W, Ketteler M. Magnesium basics. Clinical Kidney Journal. 2012;5(Suppl_1):i3-i14.

35. Zeng Z, Stanford N, Davies CHJ, Nie J-F, Birbilis N. Magnesium extrusion alloys: a review of developments and prospects. International Materials Reviews. 2019;64(1):27-62.

36. Maguire ME, Cowan JA. Magnesium chemistry and biochemistry. Biometals. 2002;15(3):203-10.

37. Ng WF, Chiu KY, Cheng FT. Effect of pH on the in vitro corrosion rate of magnesium degradable implant material. Materials Science and Engineering: C. 2010;30(6):898-903.

38. Al-Ghamdi SMG, Cameron EC, Sutton RAL. Magnesium Deficiency: Pathophysiologic and Clinical Overview. American Journal of Kidney Diseases. 1994;24(5):737-52.

39. Wolff J. The law of bone remodelling: Springer Science & Business Media; 2012.

40. Kumar S, Katyal P. Factors affecting biocompatibility and biodegradation of magnesium based alloys. Materials Today: Proceedings. 2021.

41. Kawamura N, Nakao Y, Ishikawa R, Tsuchida D, Iijima M. Degradation and Biocompatibility of AZ31 Magnesium Alloy Implants In Vitro and In Vivo: A Micro-Computed Tomography Study in Rats. Materials. 2020;13(2):473.

42. Song G. Control of biodegradation of biocompatable magnesium alloys. Corrosion Science. 2007;49(4):1696-701.

43. Witte F, Hort N, Vogt C, Cohen S, Kainer KU, Willumeit R, et al. Degradable biomaterials based on magnesium corrosion. Current Opinion in Solid State and Materials Science. 2008;12(5):63-72.

44. Sanchez AHM, Luthringer BJC, Feyerabend F, Willumeit R. Mg and Mg alloys: How comparable are in vitro and in vivo corrosion rates? A review. Acta Biomaterialia. 2015;13:16-31.

45. Grün NG, Holweg P, Tangl S, Eichler J, Berger L, van den Beucken JJJP, et al. Comparison of a resorbable magnesium implant in small and large growing-animal models. Acta Biomaterialia. 2018;78:378-86.

46. Gu X, Zheng Y, Cheng Y, Zhong S, Xi T. In vitro corrosion and biocompatibility of binary magnesium alloys. Biomaterials. 2009;30(4):484-98.

47. Kuhlmann J, Bartsch I, Willbold E, Schuchardt S, Holz O, Hort N, et al. Fast escape of hydrogen from gas cavities around corroding magnesium implants. Acta Biomaterialia. 2013;9(10):8714-21.

48. Jin L, Wu J, Yuan G, Chen T. In vitro study of the inflammatory cells response to biodegradable Mg-based alloy extract. PLOS ONE. 2018;13(3):e0193276.

49. Amerstorfer F, Fischerauer SF, Fischer L, Eichler J, Draxler J, Zitek A, et al. Long-term in vivo degradation behavior and near-implant distribution of resorbed elements for magnesium alloys WZ21 and ZX50. Acta Biomaterialia. 2016;42:440-50.

50. Kirkland NT. In Vitro Assessment of the Physiological Biocorrosion Behaviour of Magnesium-Based Biomaterials. 2011.

51. Feng A, Han Y. The microstructure, mechanical and corrosion properties of calcium polyphosphate reinforced ZK60A magnesium alloy composites. Journal of Alloys and Compounds. 2010;504(2):585-93.

52. Wang G, Li J, Zhang W, Xu L, Pan H, Wen J, et al. Magnesium ion implantation on a micro/nanostructured titanium surface promotes its bioactivity and osteogenic differentiation function. Int J Nanomedicine. 2014;9:2387-98.

53. Azmat A, Tufail M, Chandio AD. Synthesis and Characterization of Ti-Sn Alloy for Orthopedic Application. Materials. 2021;14(24):7660.

54. Myrissa A, Agha NA, Lu Y, Martinelli E, Eichler J, Szakács G, et al. In vitro and in vivo comparison of binary Mg alloys and pure Mg. Materials Science and Engineering: C. 2016;61:865-74.

55. Torroni A, Xiang C, Witek L, Rodriguez ED, Flores RL, Gupta N, et al. Histo-morphologic characteristics of intra-osseous implants of WE43 Mg alloys with and without heat treatment in an in vivo cranial bone sheep model. J Craniomaxillofac Surg. 2018;46(3):473-8.

56. Mraied H, Wang W, Cai W. Influence of chemical heterogeneity and microstructure on the corrosion resistance of biodegradable WE43 magnesium alloys. Journal of Materials Chemistry B. 2019;7(41):6399-411.

57. Liu C, Ren Z, Xu Y, Pang S, Zhao X, Zhao Y. Biodegradable magnesium alloys developed as bone repair materials: a review. Scanning. 2018;2018.

58. Miller PL, Shaw BA, Wendt RG, Moshier WC. Assessing the Corrosion Resistance of Nonequilibrium Magnesium-Yttrium Alloys. Corrosion. 1995;51(12).

59. Qiao Z, Shi Z, Hort N, Zainal Abidin NI, Atrens A. Corrosion behaviour of a nominally high purity Mg ingot produced by permanent mould direct chill casting. Corrosion Science. 2012;61:185-207.

60. Han P, Cheng P, Zhang S, Zhao C, Ni J, Zhang Y, et al. In vitro and in vivo studies on the degradation of high-purity Mg (99.99wt.%) screw with femoral intracondylar fractured rabbit model. Biomaterials. 2015;64:57-69.

61. Li N, Zheng Y. Novel Magnesium Alloys Developed for Biomedical Application: A Review. Journal of Materials Science & Technology. 2013;29(6):489-502.

62. Chaya A, Yoshizawa S, Verdelis K, Myers N, Costello BJ, Chou D-T, et al. In vivo study of magnesium plate and screw degradation and bone fracture healing. Acta Biomaterialia. 2015;18:262-9.

63. Lu Y, Bradshaw AR, Chiu YL, Jones IP. Effects of secondary phase and grain size on the corrosion of biodegradable Mg–Zn–Ca alloys. Materials Science and Engineering: C. 2015;48:480-6.

64. Chen J, Tan L, Yu X, Etim IP, Ibrahim M, Yang K. Mechanical properties of magnesium alloys for medical application: A review. Journal of the Mechanical Behavior of Biomedical Materials. 2018;87:68-79.

65. Cai S, Lei T, Li N, Feng F. Effects of Zn on microstructure, mechanical properties and corrosion behavior of Mg–Zn alloys. Materials Science and Engineering: C. 2012;32(8):2570-7.

66. Wu G, Lin X, Liu Y, Peng J, Huang J, editors. Biosynthesis of Red Elemental Selenium Protein. E3S Web of Conferences; 2019: EDP Sciences.

67. Eichner K, Kappert HF. Zahnmedizinische Werkstoffe und ihre Verarbeitung. 8

ed. Stuttgart: Georg Thieme Verlag KG; 2015.

68. Liu X, Chen S, Tsoi JKH, Matinlinna JP. Binary titanium alloys as dental implant materials-a review. Regen Biomater. 2017;4(5):315-23.

69. Nihei T, Ohashi K, Hattori M, Imazato S. A surveillance study of the demand of titanium and titanium alloys in Japan. Dent Mater J. 2020;39(1):9-11.

70. Long M, Rack HJ. Titanium alloys in total joint replacement--a materials science perspective. Biomaterials. 1998;19(18):1621-39.

71. Liu Z, Thompson GE. Formation of Porous Anodic Oxide Film on Titanium in Phosphoric Acid Electrolyte. Journal of Materials Engineering and Performance. 2015;24(1):59-66.

72. Soares FMS, Elias CN, Monteiro ES, Coimbra MER, Santana AIC. Galvanic Corrosion of Ti Dental Implants Coupled to CoCrMo Prosthetic Component. Int J Biomater. 2021;2021:1313343-.

73. Biehl V, Breme J. Metallic Biomaterials. Materialwissenschaft und Werkstofftechnik. 2001;32(2):137-41.

74. Nagels J, Stokdijk M, Rozing PM. Stress shielding and bone resorption in shoulder arthroplasty. Journal of Shoulder and Elbow Surgery. 2003;12(1):35-9.

75. Denard PJ, Raiss P, Gobezie R, Edwards TB, Lederman E. Stress shielding of the humerus in press-fit anatomic shoulder arthroplasty: review and recommendations for evaluation. Journal of Shoulder and Elbow Surgery. 2018;27(6):1139-47.

76. Rack HJ, Qazi JI. Titanium alloys for biomedical applications. Materials Science and Engineering: C. 2006;26(8):1269-77.

77. Sun ZL, Wataha JC, Hanks CT. Effects of metal ions on osteoblast-like cell metabolism and differentiation. Journal of Biomedical Materials Research. 1997;34(1):29-37.

78. Le Guéhennec L, Soueidan A, Layrolle P, Amouriq Y. Surface treatments of titanium dental implants for rapid osseointegration. Dental Materials. 2007;23(7):844-54.

79. Rüdinger K. Titan und Titanlegierungen. Materialwissenschaft und Werkstofftechnik. 1978;9(5):181-8.

80. Morlock M, Jäger M. Endoprothetik des älteren Menschen. Der Orthopäde. 2017;46(1):4-17.

81. Elias C, Lima J, Valiev R. Biomedical applications of titanium and its alloys. JOM: the journal of the Minerals, Metals & Materials Society. 2008;60:46-9.

82. Liu X, Chen S, Tsoi JKH, Matinlinna JP. Binary titanium alloys as dental implant materials—a review. Regen Biomater. 2017;4(5):315-23.

83. Smith DC, Lugowski S, McHugh A, Deporter D, Watson PA, Chipman M. Systemic metal ion levels in dental implant patients. International Journal of Oral & Maxillofacial Implants. 1997;12(6).

84. Narayan R. Fundamentals of medical implant materials. ASM handbook. 2012.

85. Elmrabet NM. Corrosion control of magnesium for stent applications: University of Nottingham; 2017.

86. Jacobs JJ, Gilbert JL, Urban RM. Current Concepts Review - Corrosion of Metal Orthopaedic Implants*. JBJS. 1998;80(2).

87. Yu M. Microstructure, corrosion behavior, mechanical property and biocompatibility of compression-molded zinc-nanodiamond composites as a bio-implant material: Drexel University; 2014.

88. Umeda J, Nakanishi N, Kondoh K, Imai H. Surface potential analysis on initial galvanic corrosion of Ti/Mg-Al dissimilar material. Materials Chemistry and Physics. 2016;179:5-9.

89. Song G, Atrens A. Understanding Magnesium Corrosion—A Framework for Improved Alloy Performance. Advanced Engineering Materials. 2003;5(12):837-58.

90. Zhang E, Chen H, Shen F. Biocorrosion properties and blood and cell compatibility of pure iron as a biodegradable biomaterial. Journal of Materials Science: Materials in Medicine. 2010;21(7):2151-63.

91. Song S, Song G-L, Shen W, Liu M. Corrosion and electrochemical evaluation of coated magnesium alloys. Corrosion, The Journal of Science and Engineering. 2012;68(1):015005-1--12.

92. Song G. Recent progress in corrosion and protection of magnesium alloys. Advanced engineering materials. 2005;7(7):563-86.

93. Nasr Azadani M, Zahedi A, Bowoto OK, Oladapo BI. A review of current challenges and prospects of magnesium and its alloy for bone implant applications. Progress in Biomaterials. 2022;11(1):1-26.

94. Guo Y, Sealy MP, Guo C. Significant improvement of corrosion resistance of biodegradable metallic implants processed by laser shock peening. CIRP Annals. 2012;61(1):583-6.

95. Sealy MP, Guo YB, Caslaru RC, Sharkins J, Feldman D. Fatigue performance of biodegradable magnesium–calcium alloy processed by laser

shock peening for orthopedic implants. International Journal of Fatigue. 2016;82:428-36.

96. Rahman M, Dutta NK, Roy Choudhury N. Magnesium Alloys With Tunable Interfaces as Bone Implant Materials. Front Bioeng Biotechnol. 2020;8.

97. Breme H, Biehl V, Reger N, Gawalt E. Chapter 1a Metallic Biomaterials: Introduction. In: Murphy W, Black J, Hastings G, editors. Handbook of Biomaterial Properties. New York, NY: Springer New York; 2016. p. 151-8.

98. Agarwal S, Curtin J, Duffy B, Jaiswal S. Biodegradable magnesium alloys for orthopaedic applications: A review on corrosion, biocompatibility and surface modifications. Materials Science and Engineering: C. 2016;68:948-63.

99. Asri RIM, Harun WSW, Samykano M, Lah NAC, Ghani SAC, Tarlochan F, et al. Corrosion and surface modification on biocompatible metals: A review. Materials Science and Engineering: C. 2017;77:1261-74.

100. Rossi MC, Resendiz LR, Borrás VA. Magnesium in Synthesis of Porous and Biofunctionalized Metallic Materials. 2022.

101. Kraus T, Fischerauer S, Treichler S, Martinelli E, Eichler J, Myrissa A, et al. The influence of biodegradable magnesium implants on the growth plate. Acta Biomaterialia. 2018;66:109-17.

102. Lambotte A. L'utilisation du magnesium comme materiel perdu dans l'osteosynthèse. Bull Mem Soc Nat Chir. 1932;28(3):1325-34.

103. Verbrugge J. Le Matériel métallique résorbable en chirurgie osseuse, par Jean Verbrugge: Masson; 1934.

104. Kačarević ŽP, Rider P, Elad A, Tadic D, Rothamel D, Sauer G, et al. Biodegradable magnesium fixation screw for barrier membranes used in guided bone regeneration. Bioactive Materials. 2022;14:15-30.

105. Witte F, Kaese V, Haferkamp H, Switzer E, Meyer-Lindenberg A, Wirth CJ, et al. In vivo corrosion of four magnesium alloys and the associated bone response. Biomaterials. 2005;26(17):3557-63.

106. Wirth T, Syed Ali M, Rauer C, Süβ D, Griss P, Syed Ali S. The blood supply of the growth plate and the epiphysis: a comparative scanning electron microscopy and histological experimental study in growing sheep. Calcified tissue international. 2002;70(4).

107. Kraus T, Fischerauer SF, Hänzi AC, Uggowitzer PJ, Löffler JF, Weinberg AM. Magnesium alloys for temporary implants in osteosynthesis: In vivo studies of their degradation and interaction with bone. Acta Biomaterialia. 2012;8(3):1230-8.

108. Noviana D, Paramitha D, Ulum MF, Hermawan H. The effect of hydrogen gas evolution of magnesium implant on the postimplantation mortality of rats. J Orthop Translat. 2015;5:9-15.